Scottish Universities Environmental Research Centre

Luminescence dating of wind-blown sands from archaeological sites in Shetland

Early Modern Farmstead, Broo Peninsula
Norse settlement, Sandwick South, Unst

February 2014

T.C. Kinnaird[1], D.C.W. Sanderson[1] and G. Bigelow[2]

[1]SUERC, East Kilbride, Scotland, UK
[2]Bates College, Lewiston, Maine

East Kilbride Glasgow G75 0QF Telephone: 01355 223332 Fax: 01355 229898

Summary

This report provides optically stimulated luminescence (OSL) results for key stratigraphies from the vicinity of a Norse house at Sandwick South (Unst), and from a farmstead at Broo, Quendale (Mainland Shetland). At both sites, the sediment sequences associated with the nearby structures record accumulations of blown-sand, potentially linked to climatic instability. David Sanderson and Gerry Bigelow visited the sites in November 2013 to sample undisturbed sand sequences associated with the built structures for OSL dating. Sampling pits were opened at both sites: at Sandwick South, the 2.1 m deep trench was positioned WSW of the Norse House; at Broo, the 1.2 m deep trench was positioned E of the main building complex, within the farmyard enclosure. During fieldwork portable OSL equipment, in combination with field spectrometry, was used to appraise luminescence stratigraphies, and identify the key units for OSL dating.

The test trench at Sandwick South was strategically positioned to examine the midden sequence in proximity to the built structure: profiling samples were collected from the lowest sands (3 samples), and from sand sequences enclosing the various midden units (7 samples), including clean, post-abandonment sands (4 samples). The field profile showed an overall increase in luminescence signals with depth, consistent with an age-depth progression. Furthermore, each of the stratigraphic breaks identified in the field, corresponded with a step in signal level, suggesting temporal breaks across the sedimentary boundaries. Four OSL dating samples were collected, along with in-situ gamma spectra to cover the key stratigraphic units. Field gamma dose rates were below 0.1 mGy a^{-1}, implying that low dose rates would be encountered from the dating samples. This is consistent with the local lithology, which is also quartz poor. Nonetheless the presence of stratigraphically progressive luminescence signals in profiling confirmed that the material contained a luminescence phase with dating potential.

Laboratory profiling confirmed that luminescence sensitivities were also low in both quartz and polymineral fractions. Quartz was present in the sediments, but when examined had very low luminescence sensitivity, which combined with low dose rates, precluded application of the quartz SAR method. Electron microscopy confirmed the presence of a high sodium feldspar fraction, which was separated and used for infra-red stimulated luminescence (IRSL) dating. Dose estimates were undertaken using an adapted SARA protocol, incorporating long overnight preheats before first measurement, to mitigate short-term fading effects (following the suggestions of Sanderson, 1988a). To accommodate the low dose rates the sediment samples were light protected and subjected to prolonged high resolution gamma spectrometry prior to mineral extraction. Thick source beta counting performed on subsamples were also conducted for extended periods. Internal alpha dose rates have been estimated on the basis of ICPMS analyses of comparable feldspars, and make a minor (~10%) contribution to the overall dose rates from this material (typically 0.4-0.5 mGy a^{-1}). Fading tests have been initiated, but so far no corrections have been applied. Using these procedures, the following chronology is suggested for the Sandwick South site: the lowest sand in the position of the test pit is dated to AD 1220 ± 120 (SUTL2603), and the mixed sand/midden dated to AD 1290 ± 80 (SUTL2602) and AD1210 ± 80 (SUTL2601). These three age estimates are indistinguishable within error, implying a rapid sediment accumulation. If they are

treated as synchronous the combined result is AD1240 ± 50. The overlying sand in this profile gives a result of AD 1770 ± 50.

At Broo, east of the main building complex and in the main farmyard enclosure, the pit provided access to undisturbed sands in contact with substrata, and to sands beneath and above a flagstone-lined drain, thereby providing TPQ and TAQ for the period of construction of the drain, and the overlying sequence of sands leading to the upper, post-abandonment sands. The field profile again showed a progression in luminescence signals with depth, with steps in signal level across the main stratigraphic breaks. Importantly, the lowest sands, which directly seal the substrate, are characterised by signal intensities an order of magnitude larger than those in the uppermost sands. As with earlier analyses from Broo, it was possible to apply the quartz SAR technique. Laboratory profiling was conducted, which verified the presence of both quartz and feldspars and corroborated the field profiling results. The quartz OSL SAR sand-based chronology obtained for the section at Broo encompasses a span from the late 14th century through to the early 18th century. The lowest sand in the section is dated at AD 1370 ± 40 (SUTL2608). The flagstone-lined drain was constructed in the period between AD 1510 ± 60 (SUTL2607) and AD 1550 ± 60 (SUTL2606). The clean sands identified in the upper part of the profile are dated to AD 1710 ± 60.

In addition to these formal samples, two samples were also dated from a test trench cut immediately NW of the building to examine a midden sequence outside the main enclosure. The section was sampled in 2012 by Zoe Outram (University of Bradford), in the absence of field spectrometry or OSL profiling equipment. In addition to the two dating samples above and beneath the midden sequence, a series of 20 bulk gamma spectrometry samples was collected to permit retrospective analysis of the external gamma dose rates. The gamma dose rates were reconstructed from 17 of these giving wet gamma dose rates of 0.90 and 0.87 mGy a^{-1}, which are comparable with the measured values recorded in the adjacent pit. Individual quartz OSL SAR ages fall in 18th century AD, implying a short period of accumulation (individual ages are AD 1720 ± 15 and AD 1780 ± 35, SUTL2576 and 2577, respectively).

Interestingly both sites show periods of significant sands accumulation in the 18th century. At Sandwick South the 12th/13th century activity falls within the period of radiocarbon dates from the site. There may be scope for further refinement if the internal activity were determined directly, and also data reviewed following a prolonged fading test. At Broo, the lowest sand extends the chronology within the vicinity of the settlement, with early 16th century dates above and below the drain corroborating an earlier determination of 1540 ± 40AD (SUTL 2441) obtained in the vicinity of the Broo II site. These new determinations thus add to the growing body of luminescence dates for windblown sands in Shetland.

Contents

List of figures

List of tables

1. Introduction

This report is concerned with optically stimulated luminescence (OSL) investigations of archaeologically-significant wind-blown sand deposits collected from excavations at Sandwick, Unst and on the Broo peninsula, Shetland. The excavations at Sandwick concern a Norse longhouse, and the excavations at Broo an Early Modern farmstead. Both excavations were directed by G. Bigelow.

1.1. Research questions

1.1.1. Sandwick South, Unst

OSL samples were collected with the aim of constraining the timing and periodicity of sand blows in and around the Norse settlement site at Sandwick South.

Figure 1-1: Oblique aerial photograph of the remains of the Norse settlement at Sandwick South, Unst. RCAHMS.

The red arrow marks the approximate position of the test pit cut in November 2013; a photograph of the test pit is shown in figure 2-1

Profiling samples were collected from the lowest unit of undisturbed sands (3 samples), and sand sequences enclosing the various midden phases (7 samples), including clean, post-abandonment sands (4 samples). Dating samples were collected from strategic positions through the section: from the undisturbed sands at the base (SUTL2603), sands above the first midden phase (SUTL2602 and SUTl2601, separated by a thin ash layer), thereby providing TAQ for the first midden phase, and the first clean sands in the section (SUTL2600).

1.1.2. Broo II, Broo Peninsula

The OSL samples were collected with a view to constraining the timing and periodicity of sand blows in and around the township of Broo (Broo peninsula, Shetland), supplementing previous OSL investigations (Kinnaird et.al. 2013a,b). Samples were collected for OSL dating and sampling from two test trenches/pits in the vicinity of the farmstead designated Broo II. The first test trench is located immediately E of the main building complex, within the main farmyard enclosure; the second is located NW of Building 1 (NE room), outside the main enclosure.

The main test pit, located in the farmyard enclosure, provided access to the lowest undisturbed sands in the sequence and the strata they overlie (3 samples), sands beneath and above a flagstone-lined drain (2 samples), thereby providing TPQ and TAQ for the period of its construction (3 samples), and the overlying sequence of

sands leading to the upper, post-abandonment sands (5 samples). Dating samples were taken at strategic positions through the pit: from the lowest horizon of undisturbed sand (SUTL2608), sands above and beneath of the drain, providing TPQ (SUTL2607) and TAQ (SUTL2606) for the period of construction, and the first clean sands in the section (SUTL2605).

In the micromorphological section (henceforth, the Outram section; Fig 2-2), samples were collected for OSL dating from sands at the base and top of the midden sequence, to temporally position the section within the wider site chronology. Samples were collected from: (i) sands [5009] which directly seal an anthropogenic layer (context [5010] and [5006]) containing charcoal, animal bone (with butchery marks), fish bone, clay pipe stems and decorated redware pottery assigned to the 17th century. Given its context, this sand potentially records the onset of the period of increased storminess that led to the eventual decline of the farmstead (Outram, 2013, pers comm.); and (ii) sands [5015] which seal cultural deposits [5014] and [5013], which have been interpreted as relating to the occupation of Broo II. This layer is believed to mark a significant sand blow event prior to the final abandonment of the site (Outram, 2013, pers comm.). A date for this accumulation, as well as for context [5009] would allow questions to be addressed including the accumulation rate for deposits in this area of the site.

2. Sampling

David Sanderson, accompanied by Gerry Bigelow, visited the archaeological sites at Quendale (Broo peninsula, Shetland) and Sandwick South (Unst), in November 2013, to collect samples for luminescence profiling and dating. At each locality, test pits were excavated, and then cleaned for sampling. Small quantities of sediment (1-5g each) were collected in a numbered petri dish from each of the profiling sample positions, with an additional 10g sample of the surrounding material recovered in a zip-seal bag. Samples for OSL measurement were collected using steel tubes inserted into the vertical face of the stratigraphy, subsequently extracted, and sealed. All OSL samples were extracted under dark cover. Sample locations were enlarged for in situ field gamma spectrometry (FGS) measurements (see below), taken using a Rainbow Multichannel Analyser coupled with a 2 × 2" NaI probe. In addition, 'bulk' samples of sediment were recovered for laboratory water content and dosimetry measurements.

Zoe Outram (University of Bradford) collected two samples from a test pit, outside of the main enclosure, at Broo II in 2013. These samples were collected with no field spectrometry, or portable OSL profiling to characterise the luminescence stratigraphy.

Sampling details, including the names assigned to each tube and bulk sample in the field, and the laboratory (SUTL) numbers assigned to each on arrival at the SUERC luminescence laboratories, are summarised in Table 2-1. Corresponding details for the profiling samples are summarised in Table 2-2.

Field no.	SUTL no.	Distance from datum/ cm	Layer	Context	Significance
Profile 1: Sandwick south section					
OSL1	2600	143	SU3	Sand above SU4	TAQ for SU4
OSL2	2601	82	?SU5/6?	Beneath ash layer	Between SU4 and SU7
OSL3	2602	74	SU6	Sand above first phase midden	TAQ for first phase midden
OSL4	2603	25	SU7/8	Sand in first phase midden	primary sand blow in this position
Profile 2: Broo II Section					
OSL5	2605	93.5		Base of top sand	
OSL6	2606	42		Above thin dark layer, on top of flag stones	TAQ for flagstone setting
OSL7	2607	31.5		Base of second sand, beneath flag stones	TQP for flagstone setting
OSL8	2608	22.5		Lowest sand in section	onset of sand deposition in this location
Zoe Outram section: Broo II					
OSL1	2576	-119	context [5009]	sand seals anthropogenic layer (contexts [5010] and [5006])	onset of sand deposition in this location
OSL2	2577	-184	context [5015]	seals cultural deposit [5014] and [5013], related to occupation of Broo	constrain periodicity of sand blow events in this section

Table 2-1: Sample descriptions, contexts, and archaeological significance of SUTL2600-2608

Field no.	Laboratory ref.	Distance from datum/ cm	Layer	Context	Significance
Profile 1: Sandwick south section					
P1/1	2604A	190		Top sand	(Turf at 210 cm)
P1/2	2604B	168			
P1/3	2604C	155		Above SU4	
P1/4	2604D	143		Just above SU4	TAQ for unit 4 (SUTL2600)
P1/5	2604E	90		Below SU4	
P1/6	2604F	82		Yellow sand	(SUTL2601)
P1/7	2604G	70	SU6	Yellow sand	Above SU7 (SUTL2602)
P1/8	2604H	23	SU7/8?	Grey sand	(SUTL2603)
P1/9	2604I	12	SU7/8	Yellow sand	
P1/10	2604J	0	Base of 7/8		

Profile 2: Broo II Section					
P2/1	2609A	113		Top of sand	
P2/2	2609B	90		Base of top sand	Just below SUTL2605
P2/3	2609C	65			
P2/4	2609D	50			
P2/5	2609E	41		Above flags	TAQ for flags (SUTL2606)
P2/6	2609F	35			
P2/7	2609G	30		Below flags, above dark layer	TPQ for flags (SUTL2607)
P2/8	2609H	24		Lowest sand	Onset of sandblow in this location (SUTL2608)
P2/9	2609I	20		Subsoil	
P2/10	2609J	10		Basal clay	

Table 2-2: Profiling sample descriptions

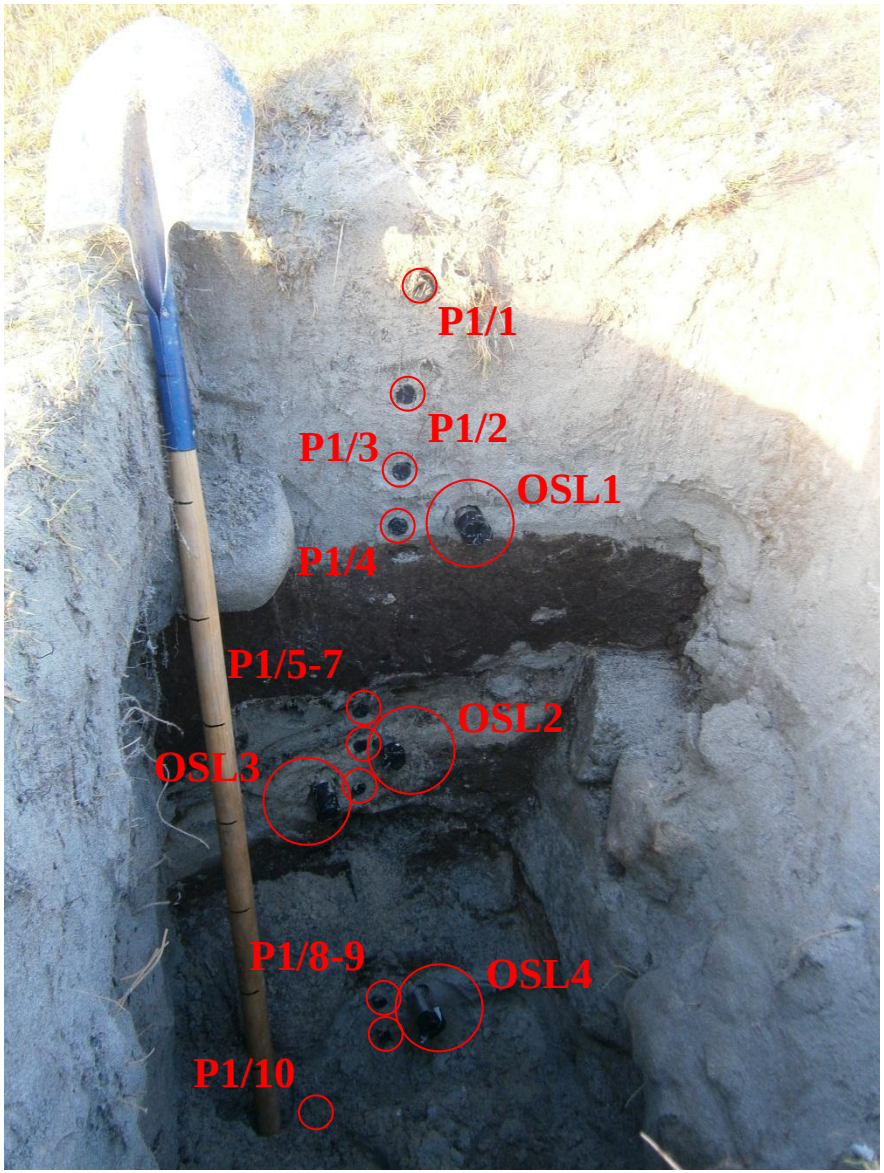

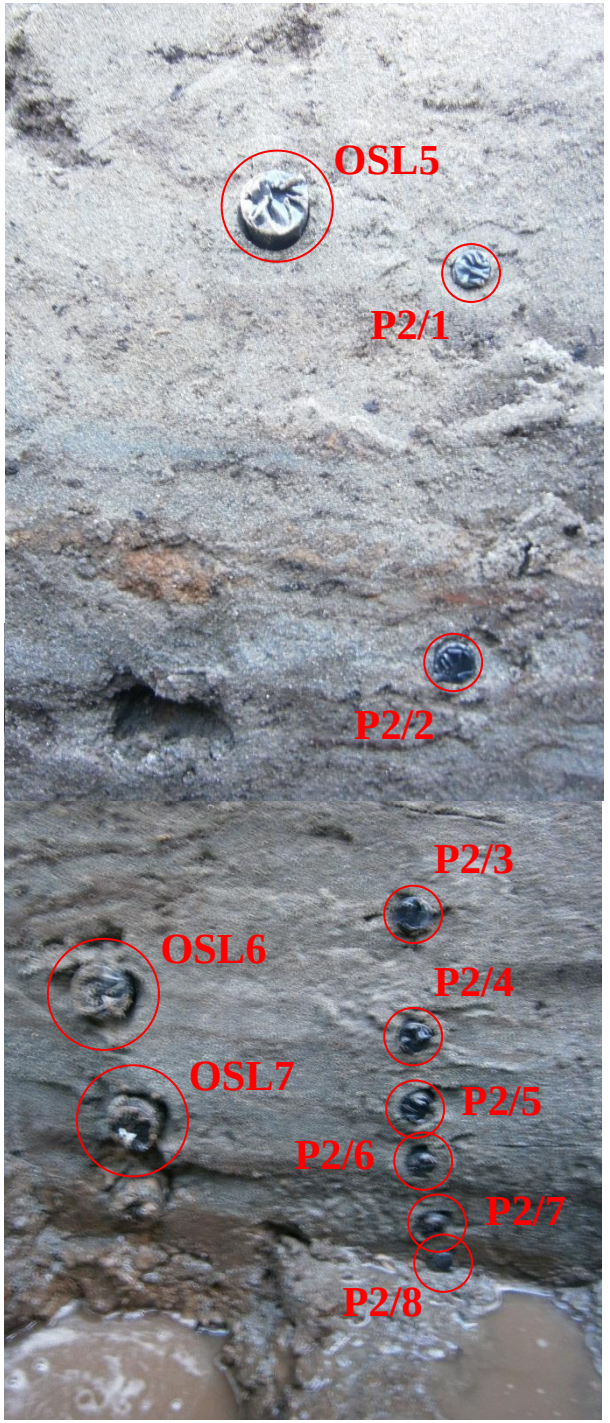

Figure 2-1: Photographs of the sampled sections: (left) Sandwick South (right) Broo II, Sanderson section

Figure 2-2: Photographs of section sampled by Zoe Outram at Broo II:
(left) Details of the main deposits/layers in the trench to the NW of the main excavation area, immediately to the NW of Building 1, NE room. The position of the OSL samples are marked; (right) Detail of section sampled for dosimetry measurements, profiling and full quartz SAR dating

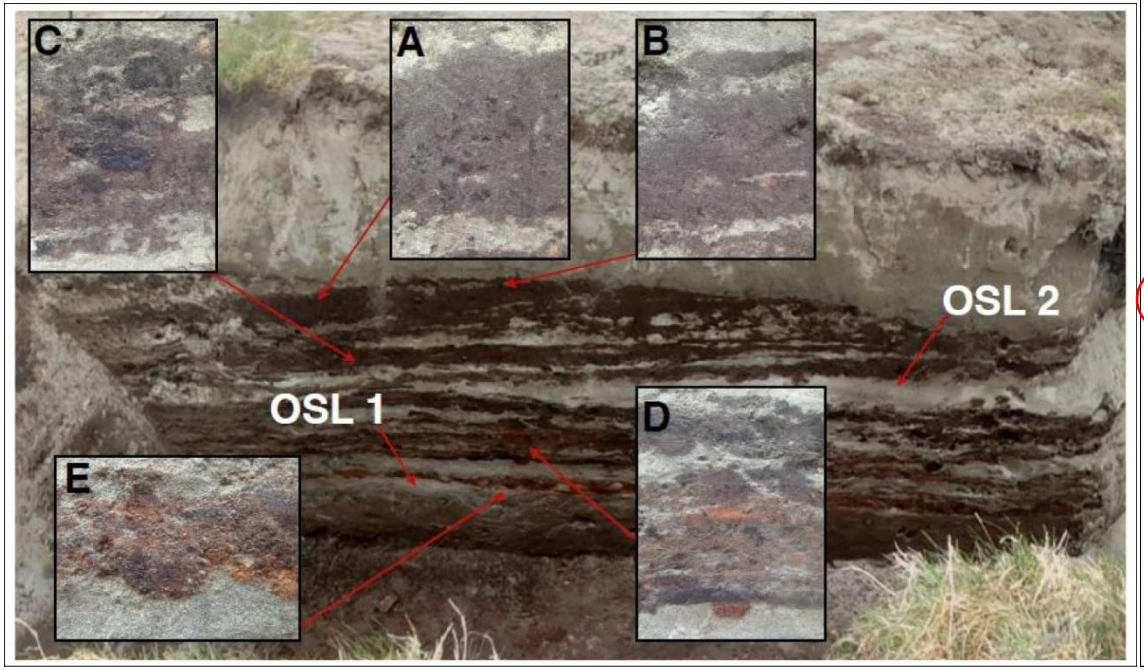

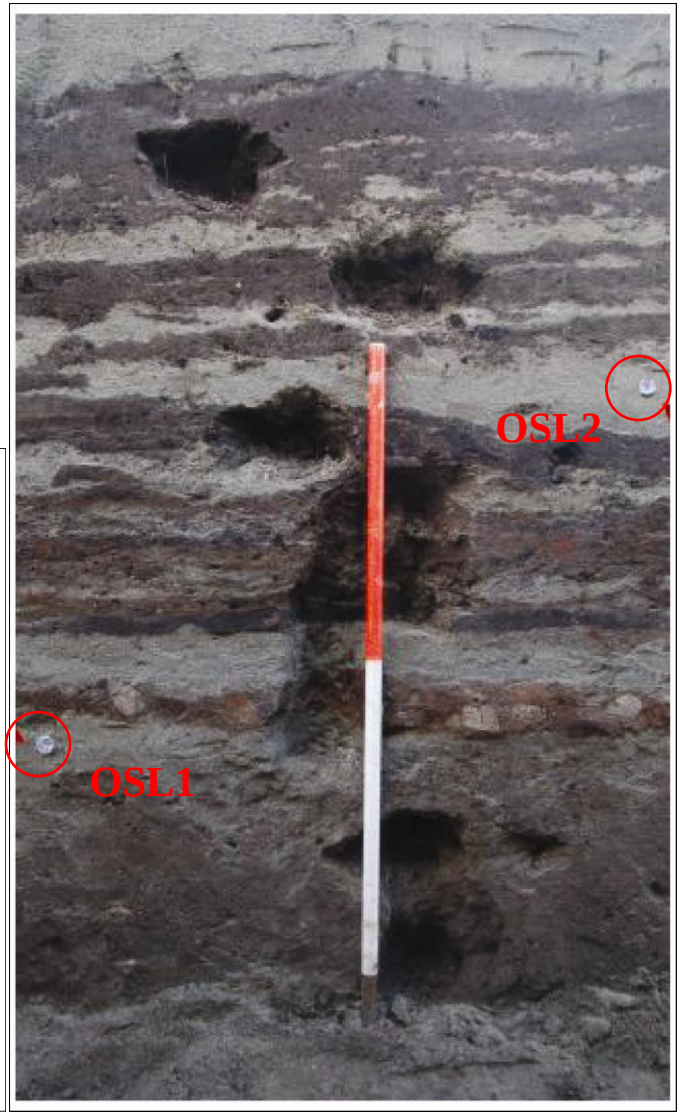

3. Field Measurements

3.1. Dose rate measurements and determinations

Field Gamma Spectrometry (FGS) measurements were made using a Health Physics Instruments Rainbow MCA with a 2"x 2" NaI probe. Prior to fieldwork, measurements were made using this system on the doped concrete reference pads at SUERC in order to provide cross-reference to dose-rate conversion factors established by Sanderson in 1986, based on comparisons with TL dosimetry in doped blocks then at the Oxford and Risø luminescence laboratories. The spectra were calibrated to the 1457 keV peak from ^{40}K, then dose rates were determined from integral counts >450 keV, >1350 keV, and the energy integral (sum of counts times energy) across all the recorded spectrum. Using this approach yielded dose rates from the pads that were within errors of expected values.

Field spectra were each measured for 300s in holes cut around the luminescence sampling positions using a towel, and calibrated to the 1461 keV peak from ^{40}K before calculation of dose rates. Table 3-1 shows the mean gamma dose rates recorded in-situ for the dating samples.

SUTL no.	FGS† / mGy a^{-1}	Description/Context	Archaeological significance
Profile 1: Sandwick south section			
2600	0.08 ± 0.01	Sand above SU4	Should give TAQ for SU4
2601	0.07 ± 0.01	Below SU4	TPQ SU4; TAQ SU7
2602	0.10 ± 0.01	Above SU7	TAQ SU7
2603	0.07 ± 0.01	Below SU7	TPQ SU7 and earliest sand in this area
Profile 2: Broo II Section			
2605	0.58 ± 0.05	Top of sand sequence	
2606	0.55 ± 0.05	Above flag	TAQ for flagstone
2607	0.54 ± 0.05	Below flag but above dark layer	TPQ for flagstone
2608	0.53 ± 0.05	Lowest sand beneath flags	Onset of sandblow at this site

Table 3-1: In situ gamma dose rates measurements made using a Health Physics Instruments Rainbow MCA with a 2"x 2" NaI probe

3.2. Field luminescence measurements

Field profiling measurements were made using a SUERC portable OSL reader, equipped with blue LEDs emitting around 470 nm and a U340 detection filter pack to detect in the region 270-380 nm, while cutting out stimulating light. Samples were presented as bulk sediment in 50mm plastic petri dishes (stored in transparent PU bags), and the natural luminescence signals were measured following an interleaved sequence of system dark count (background), infra-red stimulated luminescence and optically stimulated luminescence, similar to that described by Sanderson and Murphy (2010). All profiling samples were measured in the field. The data are presented graphically in figures 3-1 to 3-3, for the two profiles respectively, and in tabular form in appendix A.

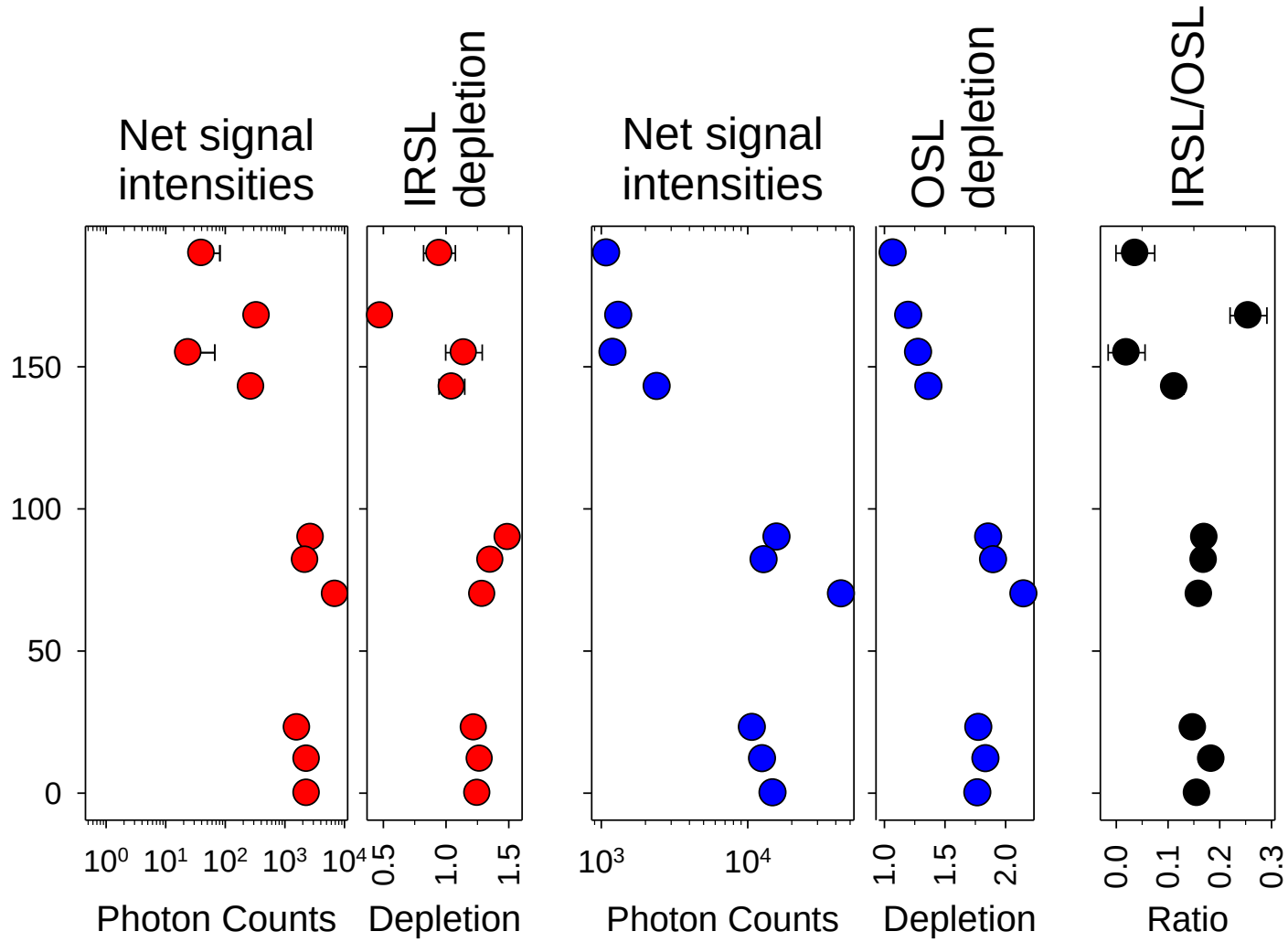

Figure 3-1: Luminescence signal intensities and depletion indices plotted vs. depth for the section sampled at Sandwick South

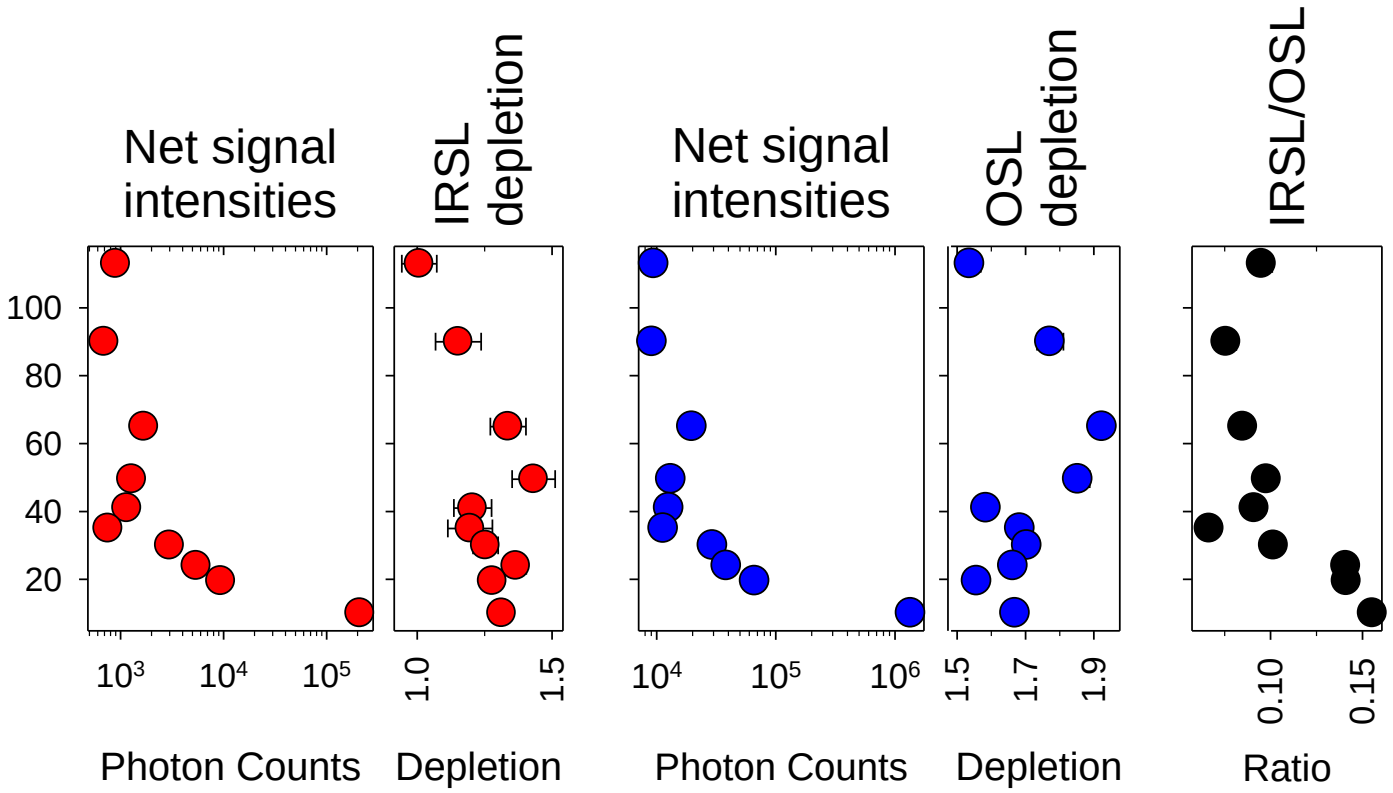

Figure 3-2: Luminescence signal intensities and depletion indices plotted vs. depth for the first of the studied sections at Broo II

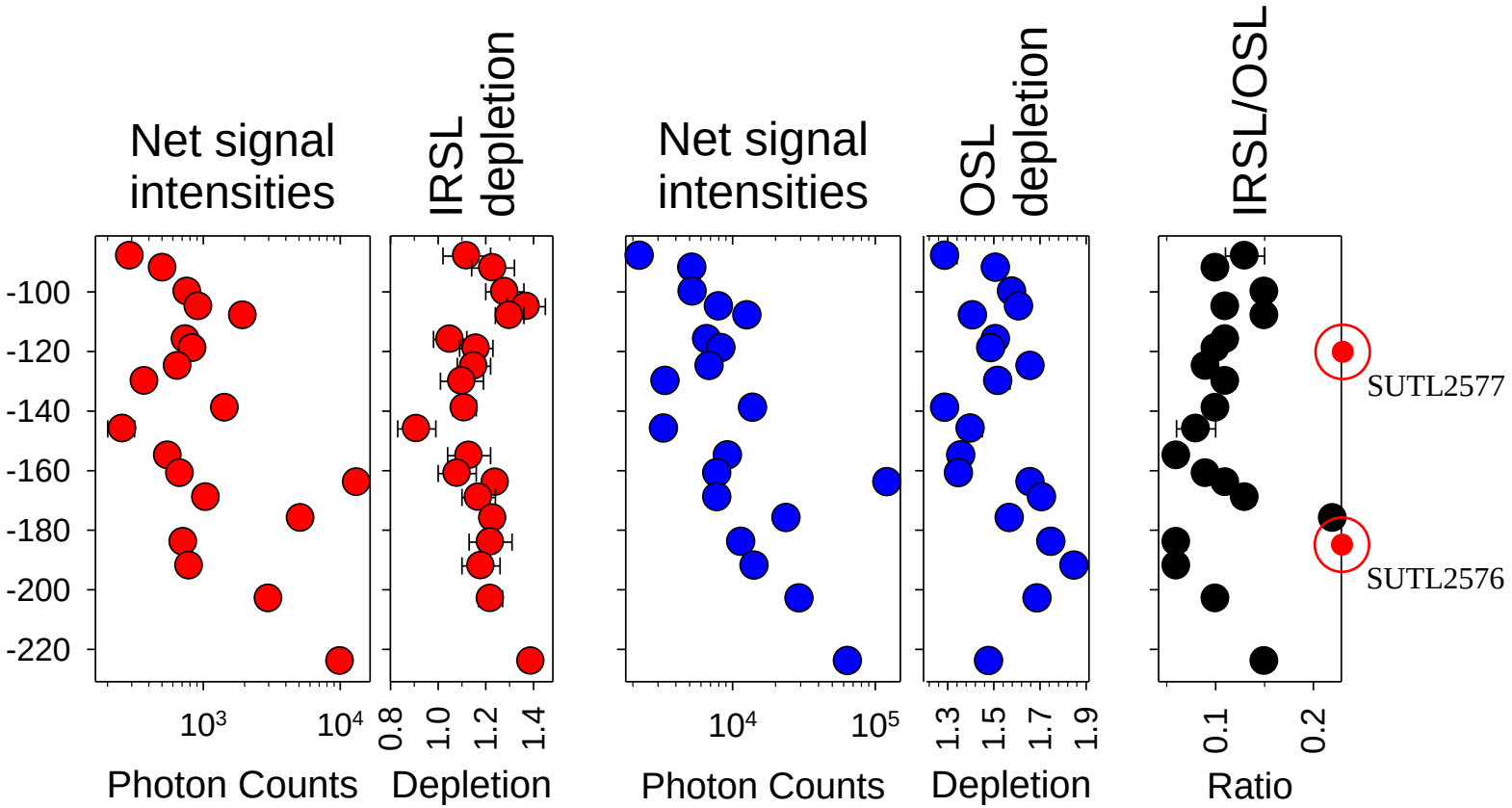

Figure 3-3: Luminescence signal intensities and depletion indices plotted vs. depth for the micro-morphological at Broo II (Outram section)

IRSL and OSL net signal intensities, depletion indices and their IRSL/OSL ratios are plotted against depth in figures 3-1 to 3-3. The interpretation of the intensities, their depletion indices and ORSL/OSL ratios has been discussed in Sanderson and Murphy (2010). Where minerals and the sediments have common sensitivities and dose rates the IRSL and OSL intensities may act as age proxies for well bleached sedimentary units, in which case inversions or discontinuities would reflect changes in initial residuality or in depositional circumstances. If sensitivity, colour or mineralogical origins change through the section, then intensities might also reflect those changes. The depletion index, which represents the proportion of signal released in the first half of the stimulation cycle relative to the second half, is an indicator of sample transparency coupled to information about whether the samples contained an inherited or single cycle signal. Higher depletion indices would indicate better bleached material. The IRSL/OSL ratio is potentially sensitive to mineralogical input changes, potentially reflecting quartz/feldspar relative contents and hence the weathering history of the sediment. These proxies can be used in combination with sedimentological observations to provide an initial interpretation of the luminescence stratigraphy.

Figure 3-1 shows the profile taken through the midden sequence sampled in proximity to the Sandwick South Norse settlement. The results are tabulated in table 3-2.

Field no.	Height / cm*	*Red*		*Blue*		IRSL : OSL ratio
		Net signal intensity	Depletion ratio	Net signal intensity	Depletion ratio	
P1/1	190	40 ± 41	0.95 ± 0.13	1089 ± 53	1.07 ± 0.06	0.04 ± 0.04
P1/2	168	337 ± 45	0.47 ± 0.05	1319 ± 54	1.20 ± 0.06	0.26 ± 0.04
P1/3	155	24 ± 43	1.14 ± 0.15	1204 ± 55	1.28 ± 0.07	0.02 ± 0.04
P1/4	143	271 ± 44	1.05 ± 0.10	2412 ± 63	1.37 ± 0.06	0.11 ± 0.02
P1/5	90	2709 ± 68	1.49 ± 0.06	15897 ± 133	1.86 ± 0.03	0.17 ± 0.00
P1/6	82	2197 ± 64	1.35 ± 0.06	12978 ± 122	1.90 ± 0.04	0.17 ± 0.01
P1/7	70	7007 ± 93	1.29 ± 0.03	43778 ± 213	2.15 ± 0.02	0.16 ± 0.00
P1/8	23	1599 ± 57	1.22 ± 0.06	10773 ± 112	1.78 ± 0.04	0.15 ± 0.01
P1/9	12	2329 ± 64	1.27 ± 0.05	12651 ± 120	1.84 ± 0.03	0.18 ± 0.01
P1/10	0	2332 ± 61	1.25 ± 0.05	14911 ± 129	1.77 ± 0.03	0.16 ± 0.00

Table 3-2: Luminescence screening results obtained using portable OSL equipment at Sandwick South (Unst)

The basal samples (P1/10 - P1/8), which may represent the primary sand blow (in the position of the test pit) show very measureable IRSL (c 2000 counts) and OSL (c 10-15 kcounts) intensities. Further up the profile, the samples enclosing the intercalated midden/sand sequence, show similar signal intensities, suggesting rapid accumulation, or re-deposition of materials of similar age. At the top of the profile, the clean sands above the dark unit SU4 show IRSL and OSL signal intensities which are one order of magnitude lower (c. 300 and 2500 counts, respectively), and lower depletion indices. The variation in signal intensities across this boundary suggests that the boundary of SU4 represents a significant age break. Further characterisation of these units, with laboratory profiling measurements, is needed to establish the extent to which luminescence sensitivity and dose rate variations contribute to the signals, in combination with age. The profiling data confirm that there are measureable trends in

luminescence properties, and that the lower units should be older than the upper material. Dating samples were taken from the lower sands (SU2603), the interdigitated midden/sand sequence (SUTL2602/2601), and at the base of the clean sands (SUTL2600).

Figure 3-2 shows the profile taken through the sediment stratigraphy at Broo, sampled in November 2013. The results are tabulated in table 3-3.

Field no.	Height / cm*	*Red*		*Blue*		IRSL : OSL ratio
		Net signal intensity	Depletion ratio	Net signal intensity	Depletion ratio	
P2/1	113	899 ± 54	1.01 ± 0.06	9461 ± 107	1.54 ± 0.03	0.10 ± 0.01
P2/2	90	694 ± 51	1.15 ± 0.08	9160 ± 106	1.77 ± 0.04	0.08 ± 0.01
P2/3	65	1686 ± 60	1.34 ± 0.07	19845 ± 148	1.92 ± 0.03	0.08 ± 0.00
P2/4	49.5	1287 ± 58	1.43 ± 0.08	13164 ± 124	1.85 ± 0.03	0.10 ± 0.00
P2/5	41	1153 ± 57	1.21 ± 0.07	12657 ± 121	1.58 ± 0.03	0.09 ± 0.00
P2/6	35	758 ± 53	1.2 ± 0.08	11374 ± 116	1.68 ± 0.03	0.07 ± 0.00
P2/7	30	3004 ± 71	1.25 ± 0.05	29544 ± 179	1.7 ± 0.02	0.10 ± 0.00
P2/8	24	5439 ± 87	1.37 ± 0.04	38600 ± 202	1.66 ± 0.02	0.14 ± 0.00
P2/9	19.5	9421 ± 108	1.28 ± 0.03	66702 ± 264	1.56 ± 0.01	0.14 ± 0.00
P2/10	10	211121 ± 464	1.31 ± 0.01	1358691 ± 1171	1.67 ± 0.00	0.16 ± 0.00

Table 3-3: Luminescence screening results obtained using portable OSL equipment at Broo (Mainland, Shetland)

The basal samples, encompassing the substrate (a clay, P2/10) and a subsoil (P2/9), are characterised by large IRSL and OSL signal intensities, the basal clay being an order of magnitude larger those obtained for the overlying archaeological materials (P2/8-P2/1). Interestingly, one can discriminate between both units, on the basis of their net signal intensities. These observations may be taken as confirmation that these layers are part of the natural substrate of the site. It is also notable that the IRSL:OSL ratio obtained for the substrate sample is substantially larger than any of those obtained from the archaeological layers above. This may indicate a greater feldspar:quartz ratio in the substrate, perhaps indicative of a different environmental origin, and/or a different weathering regime to the upper fills. Further up the section, the profiling samples representing the lowest sand layers preserved in the pit (P2/8 and P2/7) produce similar levels of IRSL and OSL signal intensities, a factor of two lower than those obtained for the basal layers, but significantly larger than the levels of signal seen in overlying sand layers. Immediately below the level of the flagstones (P2/6), and above the flagstones (P2/5-P2/3), signal intensities are substantially lower, suggesting a prominent break in stratigraphy/age before the drainage structure associated with the flagstones was constructed. Furthermore, similar signal intensities through this package, suggest a rapid accumulation. The higher OSL depletion rates obtained from these are suggestive of OSL signals that had been well bleached prior to deposition. Higher up the section, the profiling samples encasing the clean sands, are characterised by the lowest signal intensities observed in the profile. To summarise, the field profiling dataset is stratigraphically coherent, and attests to several temporal units, potentially separated by significant amounts of time.

The profile shown in figure 3-3 is taken from the micromorphological section, located immediately NW of the main excavation at Broo II, NW of Building 1 (NE room). The samples were collected for dosimetry measurements (by Zoe Outram in 2012), so that the gamma dose rate received at each of the sampling positions within this section, could be reconstructed in the absence of field spectrometry (as such the samples were collected in daylight conditions, without the protection of a dark cover). The profile indicates an overall progression in IRSL and OSL signal intensities with depth, but with substantial minima and maxima. The horizons marked by maxima in signal intensities presumably indicate re-deposition layers, containing mixed age (i.e. with residual luminescence) materials. The OSL dating samples, located at depths of 119 and 184 cm in the succession (SUTL2577 and SUTL2576, respectively), are positioned at intervals characterised by an (almost) linear increase in luminescence signals with depth.

4. Calibrated laboratory luminescence screening measurements

4.1. Methodology

All sample handling and preparation was conducted under safelight conditions in the SUERC luminescence dating laboratories. The profiling samples were wet sieved to extract the 90-250 μm fractions, which were then treated with 1M HCl for 10 minutes. The samples were split into two fractions, one for polymineral analysis and one for quartz analysis. The quartz subsample was treated with 40% HF for 40 minutes, to dissolve the less chemically resistant minerals and to etch the outer part of the grains. The HF etched material was then treated with 1 M HCl for 10 minutes to dissolve any precipitated fluorides. The grains were presented for measurement on 10 mm in diameter stainless steel discs.

Luminescence sensitivities (Photon Counts per Gy) and stored doses (Gy) were evaluated from paired aliquots of the HF-etched quartz and polymineral fractions, using Risø DA-15 automatic readers (following procedures establised in Burbidge et al., 2007; Sanderson et al., 2001; Sanderson et al., 2003). The readout cycles comprised a natural readout, followed by readout cycles for a nominal 1Gy test dose, a 5Gy regenerative dose, and a further 1Gy test dose. For the quartz samples, a 240˚C preheat was used with 60s OSL measurements using the blue LEDs. For the polymineral samples, a 260˚C preheat was followed by 60s OSL measurements using the IR LEDs at 50˚C, the IR LEDs at 225˚C (the post-IR IRSL signal), the blue LEDs at 125˚C, and a TL measurement to 500˚C.

4.2. Results

The data are presented graphically in figures 4-1 and 4-2, for the two profiles respectively. The data is tabulated in Appendix B.

Figure 4-1 illustrates the stored dose- and sensitivity-depth profiles for the stratigraphy sampled at Sandwick South. Notably, quartz OSL sensitivities are low through the section, suggesting that a signal other than the conventional OSL signal would need to be exploited in dating. Fortuitously, polymineral IRSL sensitivities are a factor larger, and IRSL stimulation at 50°C, and post-IR IRSL stimulation at 225°C, both register variations in stored dose in the sub-Gy. The basal samples (P1/10-P1/9)

returned stored dose values in excess of 100 Gy, suggesting that the bottom sands contain mixed age materials, some with large luminescence residuals. Further up the section, profile samples P1/8 to P1/5, all yield similar IRSL stored dose values, consistent with the hypothesis first postulated from the field profiling data, that this sediment accumulated rapidly or contains re-deposited materials. In contrast, profiling samples P1/4-P1/1 enclosing the upper sands, all yield lower stored dose values, further suggesting the age discontinuity across this stratigraphic boundary.

The apparent trends/maxima observed in the field profiling dataset for the section at Broo II are reproduced in the laboratory profiling dataset (Fig 4-2). The basal samples, encompassing the substrate and lowermost soil (P2/10 and P2/9, respectively), yield quartz OSL stored dose values in excess of 20 Gy, corresponding to an early Holocene age. Further up the section, the first sand horizon returned a quartz OSL stored dose of ~ 0.8 Gy (P2/8), consistent with an archaeological age. The profiling sample P2/7, collected from sands beneath the flagstones associated with the Broo II structure, yielded a similar value. Thereafter, both quartz OSL and polymineral IRSL stored dose values, return stored dose values in the range 0.5 - 0.25 Gy. This confirms the hypothesis that the flagstones mark a temporal discontinuity, with the strata either side of different age.

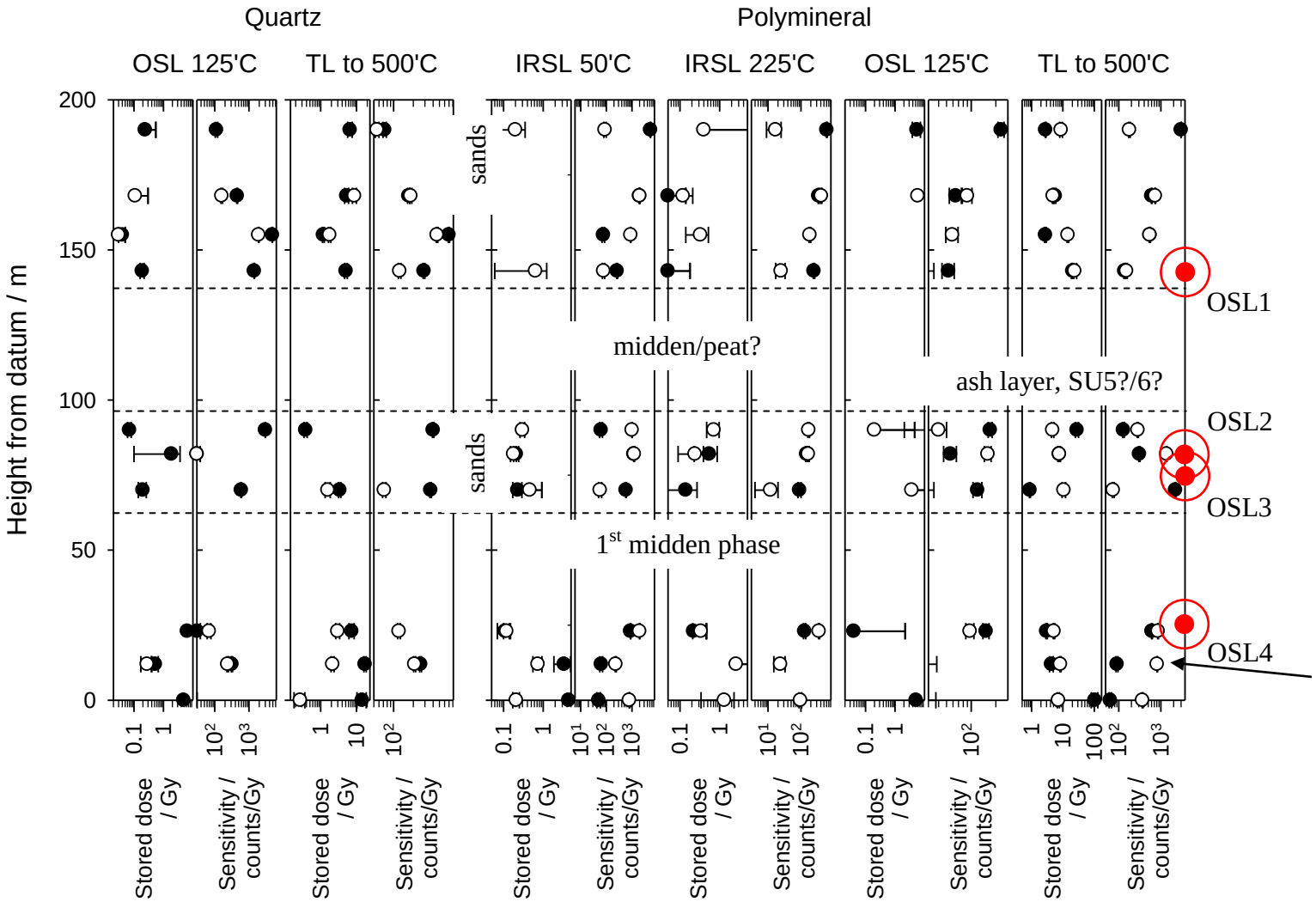

Figure 4-1: Quartz/Polymineral stored dose- and sensitivity- depth profiles for the section sampled at Sandwick South

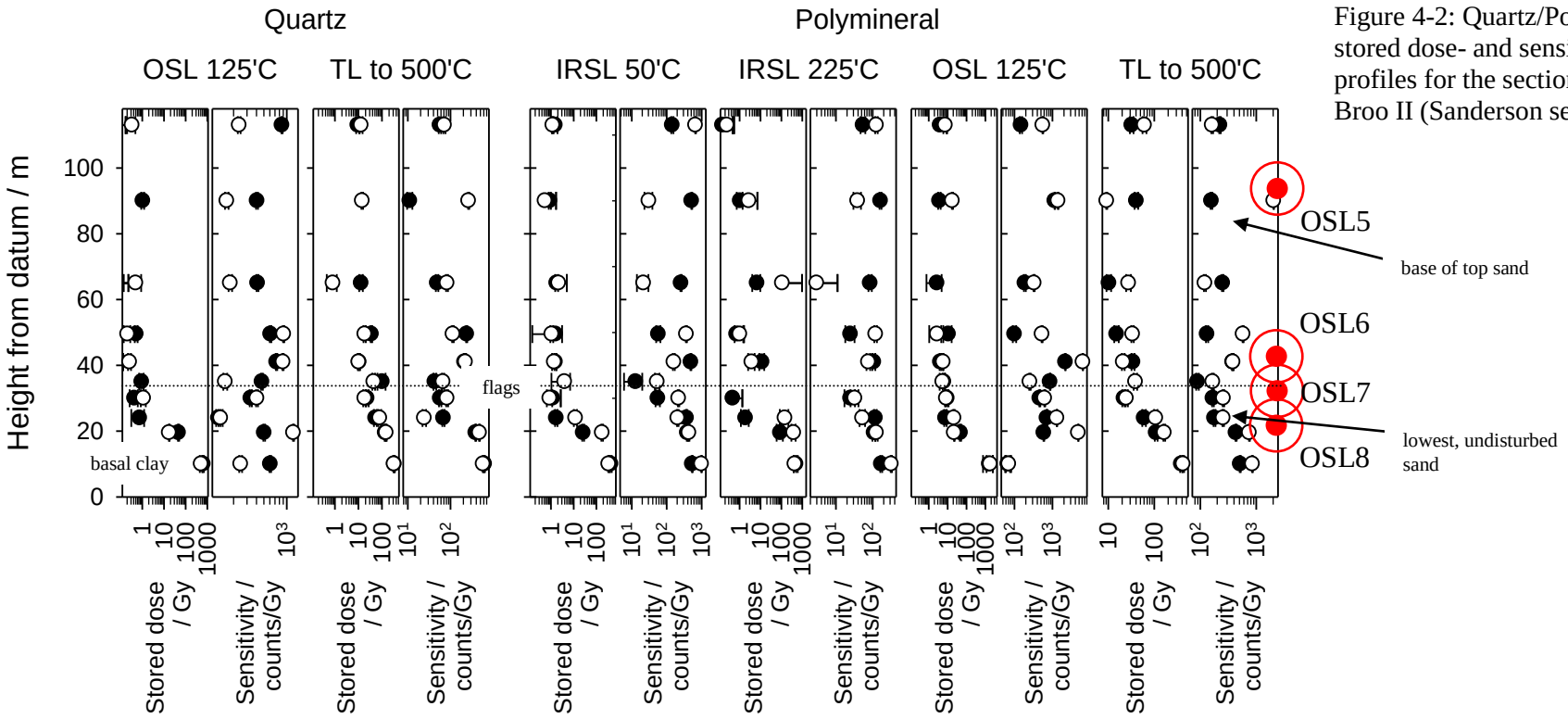

Figure 4-2: Quartz/Polymineral stored dose- and sensitivity- depth profiles for the section sampled at Broo II (Sanderson section)

5. Quartz SAR/alkali feldspar SARA measurements

5.1. Sample preparation

All sample handling and preparation was conducted under safelight conditions in the SUERC luminescence dating laboratories.

5.1.1. Water contents

Bulk samples were weighed, saturated with water and re-weighed. Following oven drying at 50 °C to constant weight, the actual and saturated water contents were determined as fractions of dry weight. These data were used, together with information on field conditions to determine water contents and an associated water content uncertainty for use in dose rate determination.

5.1.2. HRGS and TSBC Sample Preparation

Bulk quantities of material, weighing c. 150-250g, were removed from each full dating sample for environmental dose rate determinations. This material was placed in an oven to dry to constant weight. Approximately 100g and 185g quantities of dried material from each sample were weighed into HDPE pots for a high-resolution gamma spectrometry (HRGS) measurement. Samples SUTL2600-2603 and 2605/2608 were dispensed in 100g geometries; whereas samples SUTL2606-2607 were dispensed in 185g geometries. Each pot was sealed with epoxy resin and left for 3 weeks prior to measurement to allow equilibration of ^{222}Rn daughters. A further 20 g of the dried material was used in thick source beta counting (TSBC; Sanderson, 1988b).

5.1.3. Quartz/feldspar Sample Preparation

Approximately 20g of material was removed for each tube and processed for luminescence measurements, to separate sand-sized quartz and feldspar grains. The sample was wet sieved to obtain the 90-150 and 150-250 μm fractions. The 150-250 μm sub-sample was treated with 1 M hydrochloric acid (HCl) for 10 minutes, 15% hydrofluoric acid (HF) for 15 minutes, and 1 M HCl for a further 10 minutes. This etched material was then centrifuged in sodium polytungstate solutions of ~2.51, 2.58, 2.62, and 2.74 g cm^{-3}, to obtain concentrates of potassium-rich feldspars (2.51-2.58 g cm^{-3}), sodium feldspars (2.58-2.62 g cm^{-3}) and quartz plus plagioclase (2.62-2.74 g cm^{-3}). The selected quartz fraction was then subjected to further HF and HCl washes (40% HF for 40mins, followed by 1M HCl for 10 mins). All materials were dried at 50°C and transferred to Eppendorf tubes. The 15% HF-etched, 2.51-2.58 g cm^{-3} polymineral, and 40%HF-etched, 2.62-2.74 g cm^{-3} 'quartz' fractions were dispensed to 10mm stainless steel discs for measurement. 32 aliquots were produced for all samples.

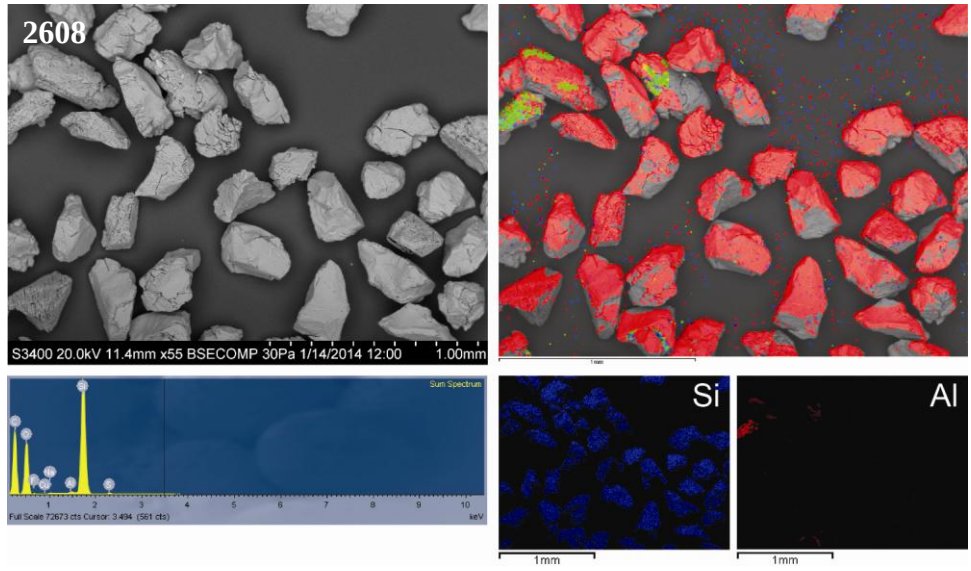

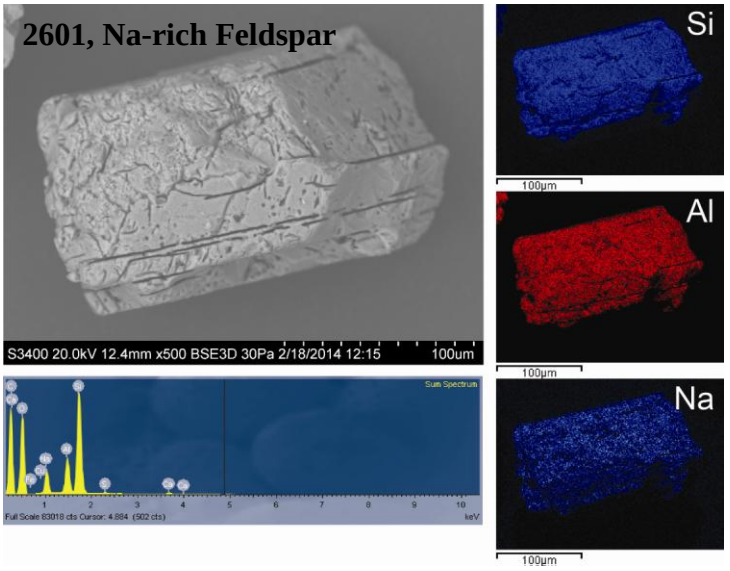

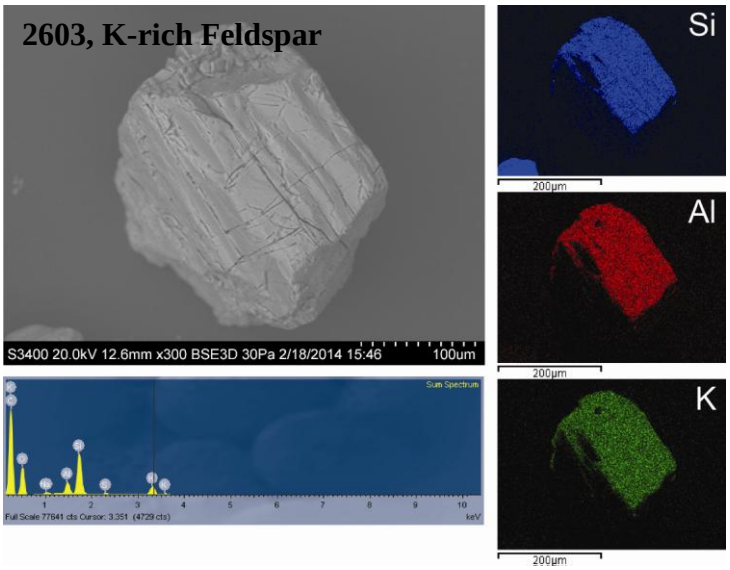

Figure 5-1: SEM images, including backscatter electron images and elemental maps for SUTL2601, 2603 and 2608

illustrating (top) the distribution of quartz (red) and alumino-silicates (green) in the 15%HF-etched, 150-250 µm fraction of SUTL2608. The alumino-silicates include both K-rich and Na-rich feldspars. Further HF and HCl washes, and density separation in sodium polytungstate concentrated the quartz phase for OSL dating

(middle) the pure Na-rich feldspars extracted from SUTL2601. The Na-rich feldspars are concentrated in the 150-250 µm, 15% HF-etched, 2.51-2.58gcm^{-3} fraction. This mineral phase is common to SUTL2600-2603

(bottom) a subordinate K-rich feldspar extracted from SUTL2603. This mineral phase has only been identified in SUTL2603. The K-rich feldspars were concentrated in the 150-250 µm, 15% HF-etched, 2.51-2.58gcm^{-3} fraction.

5.2. Measurements and determinations

5.2.1. Dose rate determinations

Dose rates were measured in the laboratory using HRGS and TSBC. Full sets of laboratory dose rate determinations were made for all samples.

HRGS measurements were performed using a 50% relative efficiency "n" type hyper-pure Ge detector (EG&G Ortec Gamma-X) operated in a low background lead shield with a copper liner. Gamma ray spectra were recorded over the 30 keV to 3 MeV range from each sample, interleaved with background measurements and measurements from SUERC Shap Granite standard in the same geometries. The sand samples collected from archaeological-significant contexts at the excavations at Broo (SUTL2576-2577, and SUTL2605-2608) were each counted for 80 ks. The sand samples collected from the archaeological-significant contexts at the excavations at Sandwick (SUTL2600-2604) were each counted for 400 ks. The spectra were analysed to determine count rates from the major line emissions from ^{40}K (1461 keV), and from selected nuclides in the U decay series (^{234}Th, ^{226}Ra + ^{235}U, ^{214}Pb, ^{214}Bi and ^{210}Pb) and the Th decay series (^{228}Ac, ^{212}Pb, ^{208}Tl) and their statistical counting uncertainties. Net rates and activity concentrations for each of these nuclides were determined relative to Shap Granite by weighted combination of the individual lines for each nuclide. The internal consistency of nuclide specific estimates for U and Th decay series nuclides was assessed relative to measurement precision, and weighted combinations used to estimate mean activity concentrations (Bq kg^{-1}) and elemental concentrations (% K and ppm U, Th) for the parent activity. These data were used to determine infinite matrix dose rates for alpha, beta and gamma radiation.

Beta dose rates were also measured directly using the SUERC TSBC system (Sanderson, 1988b). Sample count rates for the Broo sands were determined with six replicate 600 s counts for each sample, bracketed by background measurements and sensitivity determinations using the Shap Granite secondary reference material. For the Sandwick sands, sample count rates were determined from duplicate sets of measurements made on two consecutive weeks, determined with 18 and 24 replicate 600 s counts for each sample, interleaved with long background measurements and sensitivity determinations using the Shap Granite. Infinite-matrix dose rates were calculated by scaling the net count rates of samples and reference material to the working beta dose rate of the Shap Granite (6.25 ± 0.03 mGy a^{-1}). The estimated errors combine counting statistics, observed variance and the uncertainty on the reference value.

The dose rate measurements were used in combination with the assumed burial water contents, to determine the overall effective dose rates for age estimation. Cosmic dose rates were evaluated by combining latitude and altitude specific dose rates (0.18 ± 0.01 mGy a^{-1}) for the site with corrections for estimated depth of overburden using the method of Prescott and Hutton (1994).

5.2.2. Quartz SAR luminescence measurements

All measurements were conducted using a Risø DA-15 automatic reader equipped with a $^{90}Sr/^{90}Y$ β-source for irradiation, blue LEDs emitting around 470 nm and infrared (laser) diodes emitting around 830 nm for optical stimulation, and a U340 detection filter pack to detect in the region 270-380 nm, while cutting out stimulating light (Bøtter-Jensen et al., 2000). For each sample, equivalent dose determinations were made on sets of 32 aliquots per sample, using a single aliquot regeneration (SAR) sequence (cf Murray and Wintle, 2000). According to this procedure, the OSL signal level from an individual disc is calibrated to provide an absorbed dose estimate (the equivalent dose) using an interpolated dose-response curve, constructed by regenerating OSL signals by beta irradiation in the laboratory. Sensitivity changes which may occur as a result of readout, irradiation and preheating (to remove unstable radiation-induced signals) are monitored using small test doses after each regenerative dose. Each measurement is standardised to the test dose response determined immediately after its readout, to compensate for observed changes in sensitivity during the laboratory measurement sequence. For the purposes of interpolation, the regenerative doses are chosen to encompass the likely value of the equivalent (natural) dose (determined in the initial laboratory characterisation study, see section 4). A repeat dose point is included to check the ability of the SAR procedure to correct for laboratory-induced sensitivity changes (the 'recycling test'), a zero dose point is included late in the sequence to check for thermally induced charge transfer during the irradiation and preheating cycle (the 'zero cycle'), and an IR response check is included to assess the magnitude of non-quartz signals. Regenerative dose response curves were constructed using doses of 0, 1, 2, 3, 0 and 2 Gy, with a test dose of 1 Gy.

5.2.3. Alkali feldspar SARA luminescence measurements

All measurements were performed on the same equipment described above. Equivalent dose determinations were made using a single aliquot regenerative additive dose protocol combining the SARA approach (Mejdahl and Bøtter-Jensen, 1994, 1997) with longer overnight preheating as discussed by Alexander (2007) to mitigate short term fading. In the original SARA method groups of aliquots were formed with added doses, and a linear dose estimate made for each aliquot by scaling luminescence signals between the first (natural plus added dose) and a regenerated signal. Dose estimates are formed by regression of the added dose response curves to zero signal. In the modification suggested by Alexander, long overnight preheating is introduced before the first readout, so that both natural and added doses are stabilised in the manner suggested by Sanderson (1988a). Automated readout with regenerative dose pre-heated in the instrument completes the sequence. This was implemented here with sets of 32 aliquots, sub-divided into 4 groups of 8 aliquots (natural, natural + 0.5 Gy, natural + 1 Gy, natural + 1.5 Gy). Irradiations were performed using an automated Elsec irradiator equipped with a 1.85Gbq ^{90}Sr source (dose rate 1.76 Gy/min at time of the experiment). The experimental conditions were as follows: the IRSL from the natural and natural + β dose aliquots was recorded after a 16 hr preheat at 120°C; the test dose response was recorded after a 30 s preheat at 200°C; and IRSL measurements at 50°C were conducted over 60 s, with backgrounds recorded before and after stimulation.

5.2.4. Fading measurements

Fading tests were performed on 32 aliquots per sample. For each sample, 16 aliquots were given a 1 Gy dose before storage; the other 16 aliquots were given a 1 Gy dose immediately after storage. Irradiations were performed using the automated Elsec irradiator. For an initial readout the samples were stored in the dark at ambient temperatures for periods ranging between 7 and 8×10^5 s. All aliquots were given a 16hr preheat at 120°C (following the suggestions of Sanderson, 1988a), before IRSL readout at 50°C), followed by a 1 Gy test dose, pre-heat at 200°C for 30 s and a further IRSL at 50°C i.e. replicating the experiment conditions used in the SARA protocol. Following the last readout 16 aliquots per sample were again given a 1 Gy dose, before being placed in storage for a further fading test to be conducted in the future.

5.3. Results

5.3.1. Dose rates

HRGS results are shown in Table 5-1, both as activity concentrations (i.e. disintegrations per second per kilogram) and as equivalent parent element concentrations (in % and ppm), based in the case of U and Th on combining nuclide specific data assuming decay series equilibrium. The Sandwick South samples had extremely low activity, with K, U and Th concentrations ranging between 0.1 and 0.2 %, 0.2 and 0.3 ppm and 0.4 and 0.8 ppm, respectively. In contrast, the Broo II samples had K, U and Th concentrations ranging between 1.7 and 1.9 %, 1.0 and 1.2 ppm and 6.2 and 8.4 ppm, respectively.

SUTL no.	Activity Concentration[a] / Bq kg^{-1}			Equivalent Concentration[b]		
	K	U	Th	K / %	U / ppm	Th / ppm
2600	38 ± 3	2.30 ±0.05	1.78 ±0.04	0.12 ± 0.01	0.19 ± 0.00	0.44 ± 0.01
2601	39 ± 3	2.16 ±0.15	1.96 ±0.08	0.13 ± 0.01	0.17 ± 0.01	0.48 ± 0.02
2602	44 ± 3	2.14 ±0.05	1.51 ±0.03	0.14 ± 0.01	0.17 ± 0.00	0.37 ± 0.01
2603	57 ± 3	3.60 ±0.08	3.36 ±0.07	0.18 ± 0.01	0.29 ± 0.01	0.83 ± 0.02
2605	591 ± 17	13 ± 1	34 ± 1	1.91 ± 0.06	1.06 ± 0.07	8.44 ± 0.24
2606	541 ± 14	13 ± 1	26 ± 1	1.75 ± 0.04	1.02 ± 0.08	6.29 ± 0.14
2607	560 ± 16	15 ± 1	26 ± 1	1.81 ± 0.05	1.21 ± 0.05	6.45 ± 0.13
2608	550 ± 21	15 ± 2	28 ± 2	1.78 ± 0.07	1.24 ± 0.20	6.90 ± 0.46

Table 5-1: Activity and equivalent concentrations of K, U and Th determined by HRGS

[a]Shap granite reference, working values determined by David Sanderson in 1986, based on HRGS relative to CANMET and NBL standards.

[b]Activity and equivalent concentrations for U, Th and K determined by HRGS (Conversion factors based on NEA (2000) decay constants): 40K: 309.3 Bq kg^{-1} $\%K^{-1}$, 238U: 12.35 Bq kg^{-1} $ppmU^{-1}$, 232Th: 4.057 Bq kg^{-1} ppm Th^{-1}.

Infinite matrix alpha, beta and gamma dose rates from HRGS are listed for all samples in Table 5-2, together with infinite matrix beta dose rates from TSBC, and in situ gamma dose rates from FGS (section 3.1).

SUTL no.	HRGS, dry[a] / mGy a^{-1}			TSBC, dry / mGy a^{-1}	FGS, wet / mGy a^{-1}
	Alpha	Beta	Gamma		
2600	0.84 ± 0.01	0.14 ± 0.01	0.07 ± 0	0.17 ± 0.01	0.08 ± 0.01
2601	0.84 ± 0.04	0.15 ± 0.01	0.08 ± 0	0.15 ± 0.01	0.07 ± 0.01
2602	0.76 ± 0.01	0.15 ± 0.01	0.07 ± 0	0.17 ± 0.01	0.10 ± 0.01
2603	1.42 ± 0.02	0.22 ± 0.01	0.12 ± 0	0.15 ± 0.01	0.07 ± 0.01
2605	8.12 ± 0.17	1.86 ± 0.04	0.91 ± 0.02	1.81 ± 0.05	0.58 ± 0.05
2606	7.49 ± 0.25	1.78 ± 0.04	0.86 ± 0.02	1.83 ± 0.05	0.55 ± 0.05
2607	8.12 ± 0.17	1.86 ± 0.04	0.91 ± 0.02	1.84 ± 0.05	0.54 ± 0.05
2608	8.54 ± 0.65	1.85 ± 0.07	0.93 ± 0.04	1.84 ± 0.03	0.53 ± 0.05

Table 5-2: Infinite matrix dose rates determined by HRGS and TSBC.
[a]based on dose rate conversion factors in Aikten (1983) and Sanderson (1987)

The water content measurements with assumed values for the average water content during burial are given in Table 5-3. The table also lists the gamma dose rate from the HRGS after application of a water content correction. Effective dose rates to the HF etched 200 μm quartz grains are given for the gamma dose rate and beta dose rate (the mean of the TSBC and HRGS data, accounting for water content and grain size).

SUTL No.	Water Content / %			Effective Dose Rate / mGy a^{-1}		
	Fractional	Saturated	Assumed	Beta[a]	Gamma	Total[b]
2576	4.5	19.2	12 ± 7	1.45 ± 0.11	0.90 ± 0.01	2.53 ± 0.11
2577	5.4	19.0	12 ± 7	1.33 ± 0.10	0.87 ± 0.01	2.39 ± 0.11
2600	16.3	25.1	19 ± 7	0.14 ± 0.02	0.07 ± 0.00	0.39 ± 0.02
2601	10.5	25.9	19 ± 7	0.09 ± 0.01	0.07 ± 0.01	0.35 ± 0.02
2602	10.5	24.6	19 ± 7	0.13 ± 0.01	0.09 ± 0.00	0.40 ± 0.02
2603	11.6	26.6	19 ± 7	0.14 ± 0.02	0.09 ± 0.01	0.42 ± 0.02
2605	20.5	22.4	21 ± 2	1.49 ± 0.07	0.74 ± 0.02	2.41 ± 0.08
2606	17.5	21.3	21 ± 2	1.30 ± 0.06	0.62 ± 0.02	2.11 ± 0.06
2607	20.4	21.7	21 ± 2	1.33 ± 0.06	0.64 ± 0.02	2.15 ± 0.07
2608	23.4	24.1	21 ± 2	1.33 ± 0.07	0.64 ± 0.03	2.15 ± 0.08

Table 5-3: Water contents, and effective beta and gamma dose rates following water correction.
[a] Effective beta dose rate combining water content corrections with inverse grain size attenuation factors obtained by weighting the 200 μm attenuation factors of Mejdahl (1979) for K, U, and Th by the relative beta dose contributions for each source determined by Gamma Spectrometry.

5.3.2. Internal grain dosimetry

In cases where the gamma dose rate is low, such as for the samples collected at Sandwick South, the internal activity becomes increasingly important. The standard age model assumes certain values for the concentration of radionuclides within each grain. Here, an estimate of the internal alpha effective dose is made on an alpha efficiency of 6.7 % (based on Burbidge et al., in prep), and U and Th internal contents of 0.18 and 0.55, respectively. The internal alpha effective dose as calculated for the Sandwick South samples is 0.06 ± 0.03 mGy a^{-1}.

5.3.3. Quartz single aliquot equivalent dose determinations

For equivalent dose determination, data from single aliquot regenerative dose measurements were analysed using the Risø TL/OSL Viewer programme to export integrated summary files that were analysed in MS Excel and SigmaPlot. Composite dose response curves were constructed from selected discs and for each of the four preheating groups from each sample, and used to estimate equivalent dose values for each individual disc and their combined sets. Dose response curves for each of the four preheating temperature groups and the combined data were determined using a linear fit (Appendix C). The equivalent dose was then determined for each aliquot using the corresponding exponential fit parameters.

The distribution in equivalent dose values was examined using radial plotting methods (Appendix D). All samples revealed some heterogeneity in their equivalent dose distributions. Single aliquots were rejected from further analysis based on the test dose sensitivity check, SAR criteria checks, the robust mean, feldspar contamination and radial plots. Table 5-4 summarises the quality evaluation checks on the SAR data (once filtered); the mean sensitivity of each aliquot and sensitivity change, the recycling ratio and zero dose response.

SUTL No.	Sensitivity (counts/Gy)	Sensitivity change (%)	Recycling Ratio	Zero Dose (Gy)	IRSL response (%)
2576	150 ± 38	24.9 ± 6.4	0.96 ± 0.04	0.26 ± 0.16	0.73 ± 0.97
2577	112 ± 38	16.01 ± 5.39	0.97 ± 0.07	0.31 ± 0.24	2.42 ± 1.05
2605	142 ± 44	23.6 ± 7.4	0.97 ± 0.14	0.02 ± 0.03	-0.15 ± 0.89
2606	103 ± 36	17.2 ± 5.9	1.06 ± 0.07	0.10 ± 0.31	0.31 ± 1.34
2607	148 ± 53	21.1 ± 7.6	0.96 ± 0.06	-2.42 ± 2.34	0.30 ± 1.00
2608	68 ± 12	11.4 ± 1.9	0.97 ± 0.05	-0.25 ± 0.22	0.83 ± 1.25

Table 5-4: SAR quality parameters. Standard errors given.

5.3.4. Feldspar equivalent dose determinations

For equivalent dose determinations, data from the single aliquot regenerative additive dose measurements were analysed using the Risø TL/OSL Viewer programme to export integrated summary files that were analysed in MS Excel and SigmaPlot. For each sample, robust and weighted mean statistical approaches were used to appraise the distribution in normalised values obtained for each 8 aliquot set (natural, natural + β1, natural + β2 etc.). The regression line fitted through the weighted mean values intercepts the additive dose axis, and provides the stored dose for that sample (see Appendix D). Regression analysis was performed using software originally developed for TL dating (Sanderson, 1987). The regression parameters and calculated stored doses are given in Table 5-5.

SUTL no.	Regression analysis			Stored dose / Gy
	m	y	x	
2600	0.84 ± 0.14	0.10 ± 0.017	-0.11 ± 0.020	0.11 ± 0.02
2601	0.90 ± 0.04	0.33 ± 0.014	-0.37 ± 0.019	0.37 ± 0.02
2602	0.96 ± 0.07	0.32 ± 0.023	-0.33 ± 0.024	0.33 ± 0.02
2603	0.92 ± 0.12	0.35 ± 0.044	-0.38 ± 0.048	0.38 ± 0.05

Table 5-5: Parameters of *m*, *y* and *c*, (with their errors) determined using the regression analysis of SUERC software

5.3.5. Fading corrections

The mean ratio of sensitisation-independent stored to prompt normalised signals, after 10^6 s storage (after Sanderson, 1988a) from all samples is 0.98, which is within error of unity. The fading rates determined from each samples during the short tests conducted are shown in Table 5-6. On the basis of these results, and the expectations for the procedure, no fading corrections have been included in the age estimates. Subsets of all samples have been re-irradiated to facilitate further fading tests if needed.

SUTL no.	Delay prior to IRSL readout		Stored to prompt ratio
	Prompt / s	Delay / s	
2600	5.91×10^4	6.79×10^5	0.87 ± 0.06
2601	6.03×10^4	7.57×10^5	0.98 ± 0.08
2602	7.65×10^4	7.54×10^5	0.99 ± 0.08
2603	5.94×10^4	7.75×10^5	1.07 ± 0.08

Table 5-6: Fading test parameters, normalised IRSL value, and sensitisation-independent stored to prompt normalised signals for SUTL2600-2603
[†]SUTL2600-2601 irradiated to 1Gy; SUTL2603 irradiated to 0.5Gy

Spencer and Sanderson (2012) report fading rates equivalent to 1-2% per decade (registered over the 5^{th}-7^{th} decade of time following irradiation and evaluated over plateau temperature) for alkali feldspars extracted from Neolithic ceramic shreds from Pool, Orkney. Similarly, Alexander (2007) found comparable rates of fading for a range of geological feldspars including pure Na-rich feldspars.

5.3.6. Age determinations

The total dose rate is determined from the sum of the equivalent beta and gamma dose rates, and the cosmic dose rate. Age estimates are determined by dividing the equivalent stored dose by the dose rate. Uncertainty on the age estimates is given by combination of the uncertainty on the dose rates and stored doses, with an additional 5% external error. Table 5-7 lists the total dose rate, stored dose and corresponding age of the sample.

SUTL No.	Dose Rate / mGy a^{-1}	Stored Dose / Gy	Years BP	Calendar years / years AD
2576	2.53 ± 0.11	0.73 ± 0.02	0.29 ± 0.02	1720 ± 15
2577	2.39 ± 0.11	0.55 ± 0.08	0.23 ± 0.04	1780 ± 35
2600	0.45 ± 0.04*	0.11 ± 0.02	0.24 ± 0.05	1770 ± 50
2601	0.41 ± 0.04*	0.33 ± 0.01	0.8 ± 0.08	1210 ± 80
2602	0.46 ± 0.04*	0.33 ± 0.02	0.72 ± 0.08	1290 ± 80
2603	0.48 ± 0.04*	0.38 ± 0.05	0.79 ± 0.12	1220 ± 120
2605	2.41 ± 0.08	0.66 ± 0.12	0.27 ± 0.05	1740 ± 50
2606	2.11 ± 0.06	0.95 ± 0.12	0.45 ± 0.06	1560 ± 60
2607	2.15 ± 0.07	1.08 ± 0.13	0.5 ± 0.06	1510 ± 60
2608	2.15 ± 0.08	1.37 ± 0.09	0.64 ± 0.05	1370 ± 50

Table 5-7: Total dose rates, stored dose and age estimates
*including an internal alpha effective dose rate contribution (section 5.3.2)

6. Discussion and conclusions

Multiple luminescence methods, from initial luminescence screening using portable OSL equipment, through laboratory characterisation measurements, to full quartz OSL SAR dating and polymineral IRSL SARA dating, have been successfully applied to archaeologically significant windblown sands in Shetland. The key findings from each of these stages are reiterated here.

The initial luminescence screening, using portable OSL equipment, provided the first appraisal of net signal variations within the sampled sections at Sandwick South and Broo. The field profile obtained from Sandwick South showed an overall increase in luminescence signals with depth, consistent with a normal age-depth progression. Furthermore, the initial luminescence screening showed that each of the stratigraphic breaks identified in the field, corresponded with a step in signal level, suggesting large temporal breaks across sediment boundaries. Similarly, the field profile collected at Broo, showed a progression in luminescence intensities with depth, with substantial variations between each of the stratigraphic units. These field profiles were used to guide the positions of the full dating samples.

Laboratory profiling reproduced the apparent trends/maxima in the field profiling dataset. It also confirmed that the quartz from Broo had sufficient sensitivity to permit dating of all archaeological materials. In addition, it provided the first indication that the quartz mineral phase at Sandwick South would prove problematic for dating (suggesting that one would have to exploit other minerals, and luminescence signals).

Following the results of the laboratory profiling, it was decided to exploit the polymineral phase to date the archaeological materials from Sandwick South. Sample preparation concentrated a pure Na-rich feldspar in sufficient quantities for dating. Long background and sample counts were used in dosimetry measurements to increase counting statistics. A modified single aliquot regenerated additive (SARA) dose method was used to estimate an apparent dose for each dating sample. The combination of these approaches provided the following preliminary chronology: the first inundation of sands to affect this site (at the position of the test pit) occurred at AD 1220 ± 120 (SUTL2603), the intercalated sand/midden sequence was deposited AD 1290 ± 80 (SUTL2602) to AD1210 ± 80 (SUTL2601), with the latter sand inundation dated to AD 1770 ± 50 (SUTL2600). Interestingly, the statistical

combination of the former three dates (indistinguishable within error), suggests a mid-13th century age for the lower sand accumulation (AD1240 ± 50).

A more conventional dating approach was followed for the dating samples collected from Broo. The individual quartz OSL SAR dates fall into the late Medieval to Early Modern periods (see Table 5-7). Table 6-1 summaries the previous quartz OSL age determinations reported for Broo II (Kinnaird et.al. 2013a,b), together with a description of the context and their archaeological significance.

The data reported here add further to the growing body of OSL dating of windblown sands on archaeological sites in Shetland. In the Sandwick South and Broo sites the stratified sequences accompanied by luminescence profiling have produced internally coherent sets of dates which confirm the presence of sand blows in the 12th-13th century (Sandwick South), the late 14th and early 16th centuries (Broo), and 18th century AD (both sites). It is also noted that the sodium feldspar approach applied at Unst, coupled to the careful measurement of dose rates from low dose rate matrix, appears to be successful at providing sedimentary dates even from this challenging material.

SUTL No.	Context	Dose Rate / mGy a^{-1}	Stored Dose / Gy	Calendar years / years AD	Significance
2441	Loamy sand; first sand horizon in geo-archaeological trench 1; trench located outside Broo site 2, lee-ward (NE) of the building	2.39 ± 0.11	1.12 ± 0.08	AD 1540 ± 40	provide an age approximation for the sands which immediately overly the bedrock; given its contextual relationship to Broo 2, then this may provide a constraint on the initial sand blow to affect the township
2442	sand, with rare charcoal inclusions; sand completely enclosures the adjacent building	2.64 ± 0.18	0.74 ± 0.04	AD 1730 ± 25	provide terminus ante quem for abandonment of the investigated farmstead
2517	Sheet sand (wind-blown); enclosed area immediately east of the excavated Broo site	2.43 ± 0.13	0.62 ± 0.05	AD 1760 ± 30	provide terminus ante quem for abandonment, and an upper constraint on the age of the soil horizon in this section
2518		2.49 ± 0.16	0.49 ± 0.06	AD 1760 ± 25	
2519	Sheet sand (wind-blown); unenclosed area immediately south-west of the excavated Broo site	2.42 ± 0.19	0.50 ± 0.05	AD 1810 ± 25	provide terminus ante quem for abandonment
2526	2.5 m thick accumulation of aeolian sands (sample collected c. 1m above base of unit), overlying a c. 1 m thick palaeosol horizon, which in turn overlies glacial till	2.61 ± 0.11	11.48 ± 0.34	2380 ± 230 BC	provides an 'age constraint' on the initial period of aeolian activity
2527	1.05 m thick accumulation of aeolian sands (sample collected c. 5 cm above base of unit), overlying a interlocked gravel horizon; roots extend to a depth of 90 cm - reworking?; within 10 cm of cobble horizon - different dosimetry	2.67 ± 0.13	0.85 ± 0.14	AD 1690 ± 50	provides an 'age constraint' on the initial period of aeolian activity
2528	> 1.10 m thick accumulation of brown-grey sand (within upper part of dune system)	2.64 ± 0.19	0.76 ± 0.02	AD 1720 ± 20	provides an 'age constraint' on the later period of aeolian activity
2529	interbedded horizons of light and grey-sands, containing one palaeosol at a depth of c. 1m; sample taken from a depth of 3.80 m, at the base of a > 1.20 m thick accumulation of dark-grey sand	2.65 ± 0.20	9.33 ± 0.17	1510 ± 270 BC	provides an 'age constraint' on the initial period of aeolian activity
2530	interbedded dark-grey, and light-grey sands, with a palaeosol at a depth of 0.50 - 0.60 m; sample collected from > 40 m thick	2.04 ± 0.15	2.00 ± 0.07	AD 1030 ± 80	provides an 'age constraint' on the later period of aeolian activity

	accumulation of light grey sands, beneath palaeosol horizon				
2531	interbedded dark-grey and light-grey sands, with a number of shell-bearing horizons in the upper part of the sequence; sample collected at a depth of 2.02 m, in a c. 0.75 m thick accumulation of sands	3.07 ± 0.25	0.18 ± 0.04	AD 1955 ± 15*	constrains periodicity of sand blows

Table 6-1: Previous OSL age determinations determined for sediment samples collected at Broo; together with a description of their archaeological significance

7. References

Aitken, M.J., 1983, Dose rate data in SI units: PACT, v. 9, p. 69–76.

Alexander, S.A., 2007, The stability of the remnant luminescence emissions of alkali feldspar [unpublished PhD thesis thesis]: Glasgow, University of Glasgow.

Bøtter-Jensen, L., Bulur, E., Duller, G.A.T., and Murray, A.S., 2000, Advances in luminescence instrument systems: Radiation Measurements, v. 32, p. 523-528.

Burbidge, C.I., Sanderson, D.C.W., Housley, R.A., and Allsworth Jones, P., 2007, Survey of Palaeolithic sites by luminescence profiling, a case study from Eastern Europe: Quaternary Geochronology, v. 2, p. 296-302.

Kinnaird, T.C., Simpson, I., and Sanderson, D.C.W., 2013a, Luminescence dating of wind-blown sands from the Broo Peninsula, Shetland. SUERC report. http://eprints.gla.ac.uk/149096/

Kinnaird, T.C., Sanderson, D.C.W., and Simpson, I., 2013b, Luminescence investigations at Quendale (Broo Peninsula, Shetland). SUERC report. http://eprints.gla.ac.uk/110510/

Mejdahl, V., 1979, Thermoluminescence dating: Beta-dose attenuation in quartz grains Archaeometry, v. 21, p. 61-72.

Mejdahl, V., and Bøtter-Jensen, L., 1994, Luminescence dating of archaeological materials using a new technique based on single aliquot measurements: Quaternary Science Reviews, v. 13, p. 551-554.

—, 1997, Experience with the SARA OSL method: Radiation Measurements, v. 27, p. 291-294.

Murray, A.S., and Wintle, A.G., 2000, Luminescence dating of quartz using an improved single-aliquot regenerative-dose protocol: Radiation Measurements, v. 32, p. 57-73.

NEA, 2000, The JEF-2.2 Nuclear Data Library: Nuclear Energy Agency, Organisation for economic Co-operation and Development. JEFF Report, v. 17.

Prescott, J.R., and Hutton, J.T., 1994, Cosmic ray contributions to dose rates for luminescence and ESR dating: Large depths and long-term time variations: Radiation Measurements, v. 23, p. 497-500.

Sanderson, D.C.W., 1987, Thermoluminescence dating of vitrified Scottish Forts: Paisley, Paisley college.

—, 1988a, Fading of thermoluminescence in feldspars: Characteristics and corrections: International Journal of Radiation Applications and Instrumentation. Part D. Nuclear Tracks and Radiation Measurements, v. 14, p. 155-161.

—, 1988b, Thick source beta counting (TSBC): A rapid method for measuring beta dose-rates: International Journal of Radiation Applications and Instrumentation. Part D. Nuclear Tracks and Radiation Measurements, v. 14, p. 203-207.

Sanderson, D.C.W., Bishop, P., Houston, I., and Boonsener, M., 2001, Luminescence characterisation of quartz-rich cover sands from NE Thailand: Quaternary Science Reviews, v. 20, p. 893-900.

Sanderson, D.C.W., Bishop, P., Stark, M.T., and Spencer, J.Q., 2003, Luminescence dating of anthropogenically reset canal sediments from Angkor Borei, Mekong Delta, Cambodia: Quaternary Science Reviews, v. 22, p. 1111-1121.

Sanderson, D.C.W., and Murphy, S., 2010, Using simple portable OSL measurements and laboratory characterisation to help understand complex and heterogeneous

sediment sequences for luminescence dating: Quaternary Geochronology, v. 5, p. 299-305.
Spencer, J.Q.G., and Sanderson, D.C.W., 2012, Decline in firing technology or poorer fuel resources? High-temperature thermoluminescence (HTTL) archaeothermometry of Neolithic ceramics from Pool, Sanday, Orkney: Journal of Archaeological Science, v. 39, p. 3542-3552.

Appendix A: Luminescence screening measurements using the portable OSL unit

Field no.	Height / cm*	*Red*		*Blue*		IRSL : OSL ratio
		Net signal intensity	Depletion ratio	Net signal intensity	Depletion ratio	
Profile 1: Sandwick south section						
P1/1	190	40 ± 41	0.95 ± 0.13	1089 ± 53	1.07 ± 0.06	0.04 ± 0.04
P1/2	168	337 ± 45	0.47 ± 0.05	1319 ± 54	1.20 ± 0.06	0.26 ± 0.04
P1/3	155	24 ± 43	1.14 ± 0.15	1204 ± 55	1.28 ± 0.07	0.02 ± 0.04
P1/4	143	271 ± 44	1.05 ± 0.100	2412 ± 63	1.37 ± 0.06	0.11 ± 0.02
P1/5	90	2709 ± 68	1.49 ± 0.06	15897 ± 133	1.86 ± 0.03	0.17 ± 0.00
P1/6	82	2197 ± 64	1.35 ± 0.06	12978 ± 122	1.90 ± 0.04	0.17 ± 0.01
P1/7	70	7007 ± 93	1.29 ± 0.03	43778 ± 213	2.15 ± 0.02	0.16 ± 0.00
P1/8	23	1599 ± 57	1.22 ± 0.06	10773 ± 112	1.78 ± 0.04	0.15 ± 0.01
P1/9	12	2329 ± 64	1.27 ± 0.05	12651 ± 120	1.84 ± 0.03	0.18 ± 0.01
P1/10	0	2332 ± 61	1.25 ± 0.05	14911 ± 129	1.77 ± 0.03	0.16 ± 0.00
Profile 2: Sanderson, Broo II section						
P2/1	113	899 ± 54	1.01 ± 0.06	9461 ± 107	1.54 ± 0.03	0.10 ± 0.01
P2/2	90	694 ± 51	1.15 ± 0.08	9160 ± 106	1.77 ± 0.04	0.08 ± 0.01
P2/3	65	1686 ± 60	1.34 ± 0.07	19845 ± 148	1.92 ± 0.03	0.08 ± 0.00
P2/4	49.5	1287 ± 58	1.43 ± 0.08	13164 ± 124	1.85 ± 0.03	0.10 ± 0.00
P2/5	41	1153 ± 57	1.21 ± 0.07	12657 ± 121	1.58 ± 0.03	0.09 ± 0.00
P2/6	35	758 ± 53	1.2 ± 0.08	11374 ± 116	1.68 ± 0.03	0.07 ± 0.00
P2/7	30	3004 ± 71	1.25 ± 0.05	29544 ± 179	1.7 ± 0.02	0.10 ± 0.00
P2/8	24	5439 ± 87	1.37 ± 0.04	38600 ± 202	1.66 ± 0.02	0.14 ± 0.00
P2/9	19.5	9421 ± 108	1.28 ± 0.03	66702 ± 264	1.56 ± 0.01	0.14 ± 0.00
P2/10	10	211121 ± 464	1.31 ± 0.01	1358691 ± 1171	1.67 ± 0.00	0.16 ± 0.00

SUTL no.	Depth / cm	Red		Blue		IRSL : OSL ratio
		Net signal intensity	Depletion ratio	Net signal intensity	Depletion ratio	
Profile 1: Outram section, Broo II						
2577A	-88	292 ± 46	1.12 ± 0.10	2243 ± 64	1.29 ± 0.05	0.13 ± 0.02
2577B	-92	507 ± 47	1.23 ± 0.09	5238 ± 85	1.51 ± 0.04	0.10 ± 0.01
2577C	-100	766 ± 51	1.28 ± 0.08	5273 ± 85	1.58 ± 0.04	0.15 ± 0.01
2577D	-105	925 ± 54	1.37 ± 0.08	8056 ± 100	1.61 ± 0.04	0.11 ± 0.01
2577E	-108	1953 ± 61	1.30 ± 0.06	12738 ± 120	1.41 ± 0.03	0.15 ± 0.00
2577F	-116	745 ± 49	1.05 ± 0.07	6652 ± 92	1.51 ± 0.04	0.11 ± 0.01
2577G	-119	839 ± 50	1.16 ± 0.07	8376 ± 101	1.49 ± 0.03	0.10 ± 0.01
2577H	-125	652 ± 50	1.15 ± 0.07	6924 ± 94	1.66 ± 0.04	0.09 ± 0.01
2577I	-130	374 ± 47	1.10 ± 0.09	3397 ± 70	1.52 ± 0.05	0.11 ± 0.01
2577J	-139	1441 ± 57	1.11 ± 0.05	13948 ± 127	1.29 ± 0.02	0.10 ± 0.00
2577K	-146	258 ± 57	0.91 ± 0.08	3321 ± 81	1.40 ± 0.05	0.08 ± 0.02
2576A	-155	553 ± 58	1.13 ± 0.09	9305 ± 110	1.36 ± 0.03	0.06 ± 0.01
2576B	-161	677 ± 59	1.08 ± 0.08	7834 ± 104	1.35 ± 0.03	0.09 ± 0.01
2576C	-164	13221 ± 128	1.24 ± 0.02	122182 ± 355	1.66 ± 0.01	0.11 ± 0.00
2576D	-169	1049 ± 62	1.17 ± 0.07	7838 ± 102	1.71 ± 0.04	0.13 ± 0.01
2576E	-176	5155 ± 89	1.23 ± 0.04	23958 ± 164	1.57 ± 0.02	0.22 ± 0.00
2576F	-184	717 ± 60	1.22 ± 0.09	11530 ± 120	1.75 ± 0.03	0.06 ± 0.01
2576G	-192	790 ± 60	1.18 ± 0.08	14294 ± 131	1.85 ± 0.03	0.06 ± 0.00
2576H	-203	3005 ± 77	1.22 ± 0.05	29556 ± 180	1.69 ± 0.02	0.10 ± 0.00
2576I	-224	9992 ± 109	1.39 ± 0.03	64613 ± 259	1.48 ± 0.01	0.15 ± 0.00

Appendix B: Laboratory luminescence screening measurements

Depth /cm	SUTL no.	OSL at 125°C				TL to 500°C			
		Stored dose /Gy		Sensitivity / counts per Gy		Stored dose /Gy		Sensitivity / counts per Gy	
		Aliquot 1	Aliquot 2	Aliquot 1	Aliquot 2	Aliquot 1	Aliquot 2	Aliquot 1	Aliquot 2
Profile 1: Sandwick South Section									
190	2604A	0.3 ± 0.3	-	113 ± 9	-	6.7 ± 1.0		73 ± 4	56 ± 4
168	2604B	-	0.10 ± 0.20	455 ± 12	161 ± 9	5.3 ± 0.7	8.8 ± 1.1	170 ± 6	183 ± 7
155	2604C	0.04 ± 0.01	0.03 ± 0.02	4830 ± 35	1928 ± 23	1.19 ± 0.07	1.8 ± 0.1	698 ± 13	460 ± 11
143	2604D	0.19 ± 0.03	-	1434 ± 20	23 ± 8	5.1 ± 0.4	-	290 ± 8	124 ± 5
90	2604E	0.07 ± 0.01	-	3027 ± 28	-	0.38 ± 0.04	-	401 ± 10	-
82	2604F	1.90 ± 1.80	-	31 ± 7	30 ± 7	192.2± 47.7	-	25 ± 2	-
70	2604G	0.20 ± 0.06	-	596 ± 15	-	3.4 ± 0.2	1.6 ± 0.3	368 ± 9	72 ± 4
23	2604H	6.40 ± 37.4	-	31 ± 7	69 ± 8	7.4 ± 1.2	3.0 ± 0.4	46 ± 3	121 ± 5
12	2604I	0.53 ± 0.13	0.28 ± 0.11	318 ± 11	240 ± 11	17.4 ± 1.4	2.2 ± 0.2	258 ± 8	209 ± 7
0	2604J	-	-	-	23 ± 7	-	0.3 ± 0.1		24 ± 2
Profile 2: Broo II, Sanderson section									
113	2609A	0.08 ± 0.09	0.30 ± 0.10	865 ± 16	238 ± 10	9.4 ± 1.3	13.1 ± 1.8	57 ± 4	72 ± 4
90	2609B	1.06 ± 0.16	-	407 ± 12	163 ± 9	-	14.6 ± 1.1	-	266 ± 8
65	2609C	0.05 ± 0.18	0.50 ± 0.40	413 ± 12	182 ± 9	13.1 ± 2.3	0.8 ± 0.4	49 ± 3	83 ± 4
49.5	2609D	0.50 ± 0.10	0.21 ± 0.07	613 ± 14	911 ± 16	35.8 ± 2.7	18.6 ± 2.1	240 ± 7	114 ± 5
41	2609E	0.06 ± 0.07	0.26 ± 0.04	735 ± 15	894 ± 16	10.8 ± 1.0	10.4 ± 0.8	212 ± 7	225 ± 7
35	2609F	0.90 ± 0.20	-	473 ± 13	156 ± 9	103.5± 39.2	45.0 ± 5.9	43 ± 3	67 ± 4
30	2609G	0.40 ± 0.20	1.2 ± 0.3	337 ± 11	407 ± 11	23.7 ± 3.6	18.7 ± 2.7	57 ± 4	84 ± 4
24	2609H	0.80 ± 0.50	-	127 ± 9	136 ± 9	53.2 ± 7.4	81.4 ± 11.5	68 ± 4	24 ± 2
19.5	2609I	46.9 ± 3.2	17.5 ± 0.7	506 ± 13	1227 ± 18	137.7 ± 8.9	150.8 ± 8.3	389 ± 9	476 ± 10
10	2609J	648.1 ±46.0	516.7 ±67.0	608 ± 14	248 ± 11	334.3 ±16.7	324.9 ±16.4	627 ± 12	579 ± 12

Depth /cm	SUTL no.	IRSL at 50°C		post- IR IRSL at 225°C		post-IR OSL at 125°C		post-IR TL to 500°C	
		Stored dose /Gy	Sensitivity / photon counts Gy^{-1}	Stored dose /Gy	Sensitivity / photon counts Gy^{-1}	Stored dose /Gy	Sensitivity / photon counts Gy^{-1}	Stored dose /Gy	Sensitivity / photon counts Gy^{-1}
Profile 1: Sandwick South Section									
190	2604A	1.37 ± 0.18	407 ± 262	0.2 ± 0.05	91 ± 36	5.83 ± 1.8	354 ± 205	46.94±14.46	194 ± 30
168	2604B	0.73 ± 0.18	275 ± 244	1.94 ± 0.88	102 ± 62	10.85 ± 7.13	1282 ± 128	25.09±15.79	1108 ± 951
155	2604C	1.99 ± 0.2	140 ± 118	59.1 ±52.27	44 ± 42	-	260 ± 71	19.06 ± 8.68	186 ± 65
143	2604D	1.35 ± 0.27	212 ± 154	0.88 ± 0.16	73 ± 48	-	317 ± 216	24.52 ± 9.32	357 ± 225
90	2604E	1.49 ± 0.09	326 ± 165	7.87 ± 3.99	92 ± 15	5 ± 0.84	4252 ±2063	27.96 ± 6.68	382 ± 4
82	2604F	4.01 ± 2	33 ± 21	-	-	5.94 ± 0.43	562 ± 306	39.12±19.56	128 ± 39
70	2604G	1.05 ± 0.16	138 ± 82	0.47 ± 0.23	29 ± 4	9.09 ± 0.48	546 ± 81	23.41 ± 1.32	214 ± 45
23	2604H	6.91 ± 5.2	289 ± 81	75.34±73.4	86 ± 33	14.72 ± 6.97	1013 ± 296	83.94±23.59	217 ± 39
12	2604I	103.6±77.3	410 ± 22	239.3±150.7	118 ± 9	35.29±12.67	2683± 2090	137.23±27.2	594 ± 160
0	2604J	396.8 ±44.5	767 ± 227	470.1±28.6	247 ± 76	1705±106.0	69 ± 2	404.1±19.2	686 ± 170
Profile 2: Broo II, Sanderson section									
113	2609A	0.11 ± 0.09	2706 ±2615	0.4 ± 0.2	314 ± 298	5.54 ± 2.77	118 ± 114	5.79 ± 2.98	1600±1421
90	2609B	0.02 ± 0.01	1989 ± 17	0.08 ± 0.03	381 ± 36	14.85 ±8.93	78 ± 12	5.27 ± 0.41	671 ± 66
65	2609C	0.02 ± 0.01	489 ± 412	0.33 ± 0.16	187 ± 93	-	39 ± 20	8.64 ± 5.85	548 ± 1
49.5	2609D	0.64 ± 0.32	172 ± 93	0.05 ± 0.03	137 ± 112	-	40 ± 13	22.14 ±1.62	145 ± 8
41	2609E	0.3 ± 0.15	537 ± 474	3.77 ± 3.05	173 ± 86	7.02 ± 6.82	106 ± 65	16.42±11.69	206 ± 78
35	2609F	0.19 ± 0.02	1214 ± 23	0.4 ± 0.16	158 ± 9	64.8 ± 32.4	108 ± 52	7.66 ± 0.03	840 ± 532
30	2609G	0.35 ± 0.12	324 ± 267	0.14 ± 0.07	51 ± 40	3.71 ± 1.85	73 ± 47	5.83 ± 4.94	1145±1071
24	2609H	0.12 ± 0	1447 ± 558	0.28 ± 0.06	243 ± 113	22.11±22.07	125 ± 27	4.11 ± 1.08	735 ± 122
19.5	2609I	2.05 ± 1.32	150 ± 86	2.62 ± 1.31	24 ± 12	84.75±42.37	15 ± 7	6.33 ± 2.01	453 ± 362
10	2609J	2.3 ± 2.1	424 ± 373	1.32 ± 0.66	97 ± 49	5.16 ± 2.58	17 ± 10	56.02±48.82	215 ± 152

Appendix C: Dose Response Plots

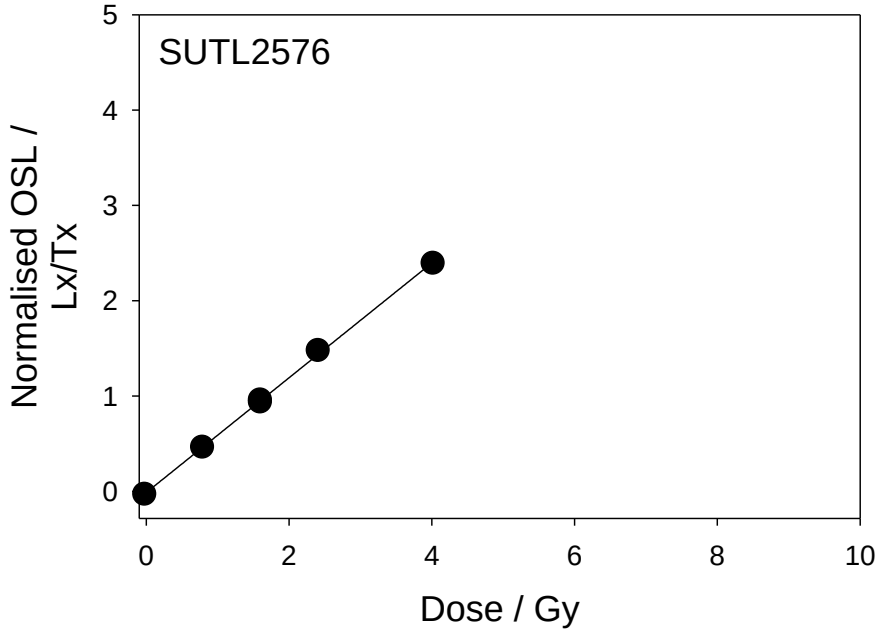

Fig C-1: Dose response for SUTL2576, 150-250 µm, 2.64 - 2.74 gcm^{-3}, 40% HF-etched polymineral fraction;

Lx = 0, 1, 2, 3 and 2 Gy; Tx = 1 Gy

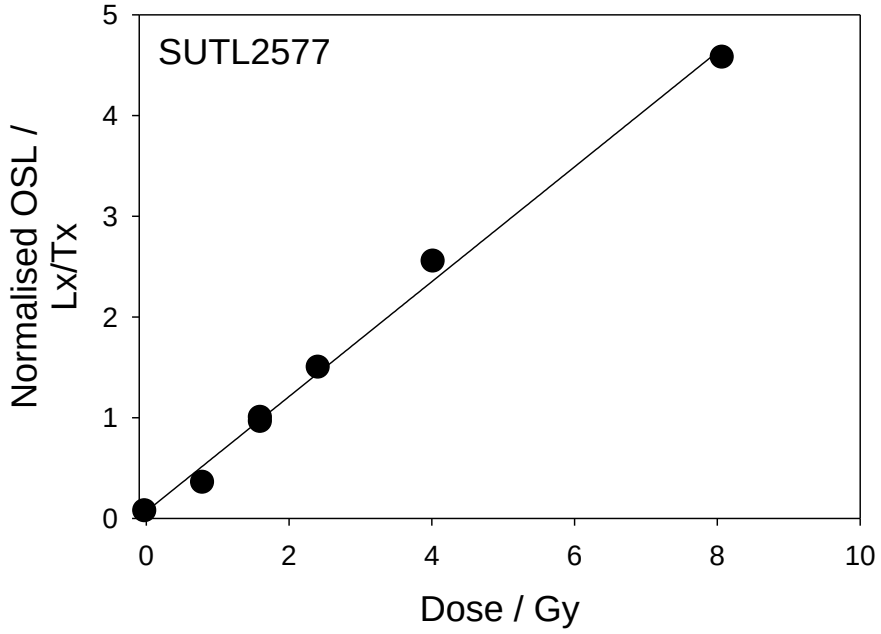

Fig C-2: Dose response for SUTL2577, 150-250 µm, 2.64 - 2.74 gcm^{-3}, 40% HF-etched polymineral fraction;

Lx = 0, 1, 2, 3 and 2 Gy; Tx = 1 Gy

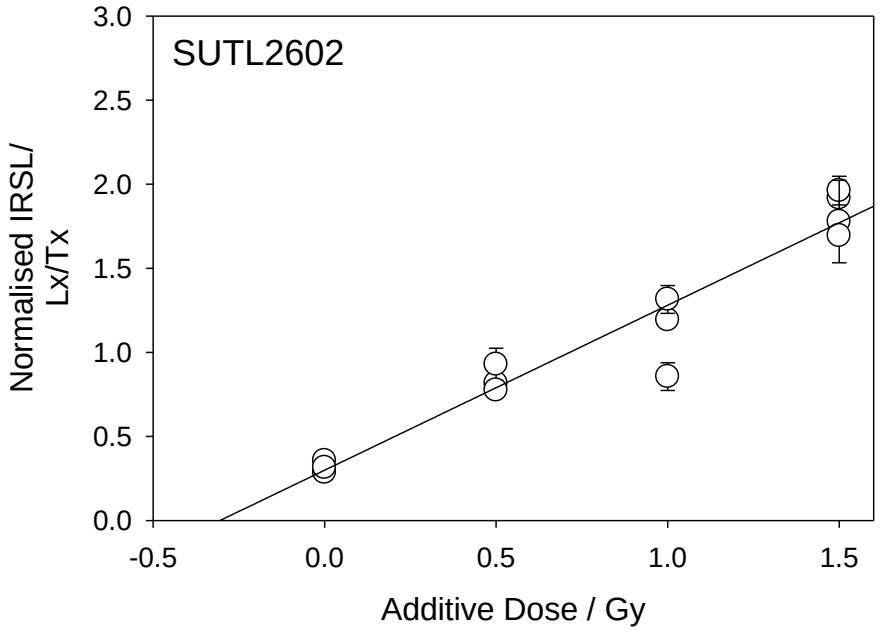

Fig C-3: Dose response for SUTL2576, 150-250 μm, 2.64 - 2.74 gcm^{-3}, 40% HF-etched polymineral fraction;

Lx = 0, 1, 2, 3 and 2 Gy; Tx = 1 Gy

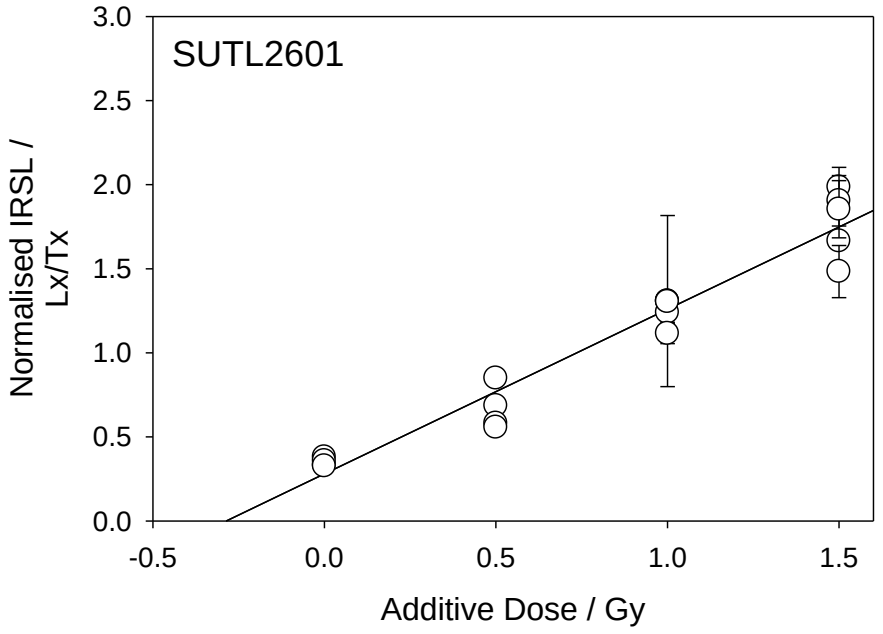

Fig C-4: Dose response for SUTL2576, 150-250 μm, 2.64 - 2.74 gcm^{-3}, 40% HF-etched polymineral fraction;

Lx = 0, 1, 2, 3 and 2 Gy; T= 1 Gy

Fig C-5: Dose response for SUTL2576, 150-250 μm, 2.64 - 2.74 gcm^{-3}, 40% HF-etched polymineral fraction;

Lx = 0, 1, 2, 3 and 2 Gy; Tx = 1 Gy

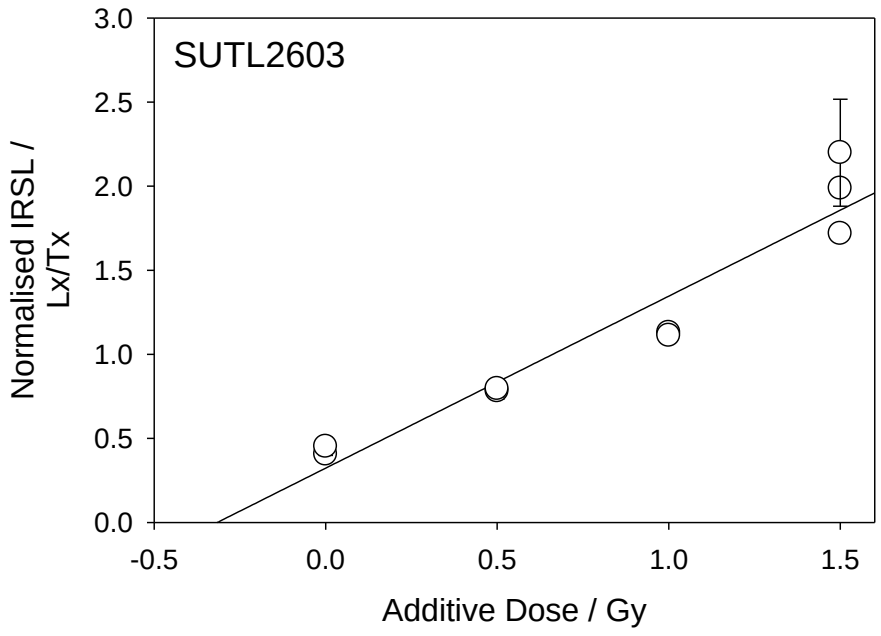

Fig C-6: Dose response for SUTL2576, 150-250 μm, 2.64 - 2.74 gcm^{-3}, 40% HF-etched polymineral fraction;

Lx = 0, 1, 2, 3 and 2 Gy; Tx = 1 Gy

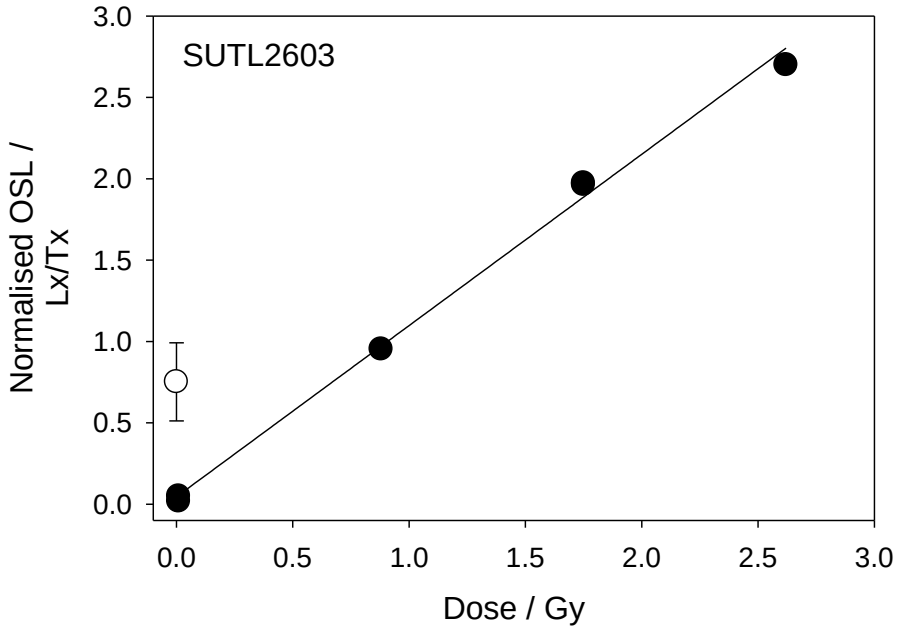

Fig C-7: Dose response for SUTL2603, 150-250 μm, 2.51-2.58 gcm^{-3} 15% HF-etched polymineral fraction;

Lx = 0, 1, 2, 3 and 2 Gy; Tx = 1 Gy

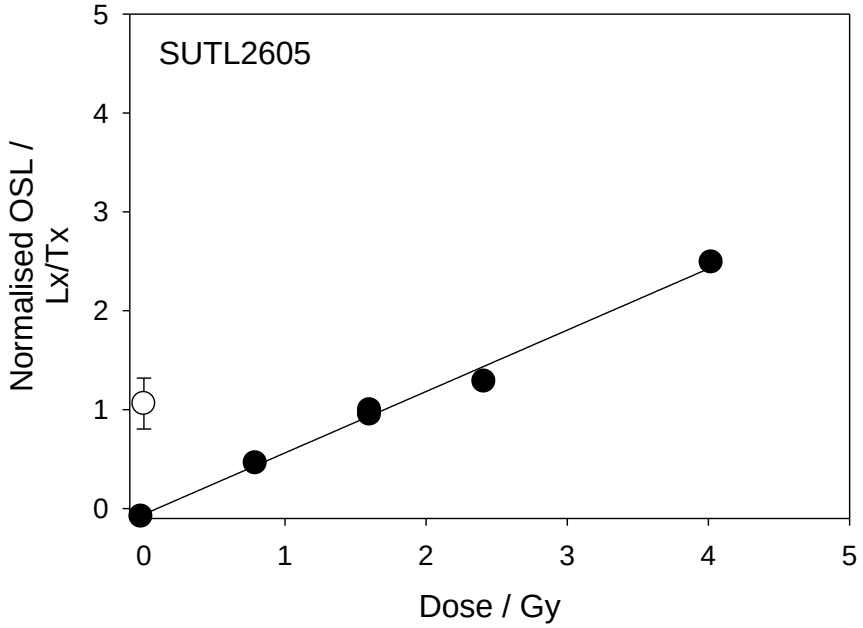

Fig C-8: Dose response for SUTL2605, 150-250 μm, 2.64-2.74 gcm^{-3} 40% HF-etched 'quartz' fraction;

Lx = 1, 2, 3 and 5 Gy; Tx = 2 Gy

Fig C-9: Dose response for SUTL2606, 150-250 μm, 2.64-2.74 gcm^{-3} 40% HF-etched 'quartz' fraction;

Lx = 1, 2, 3 and 5 Gy; Tx = 2 Gy

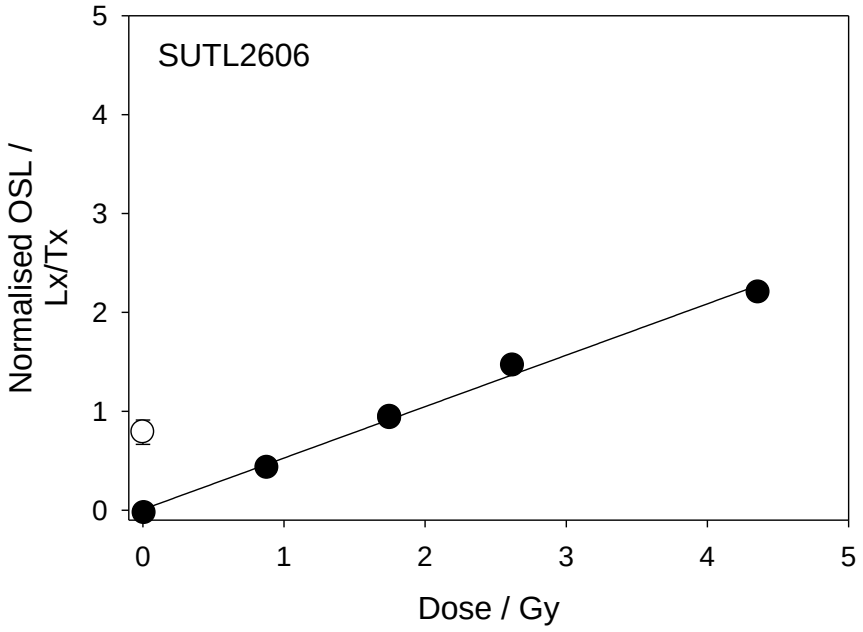

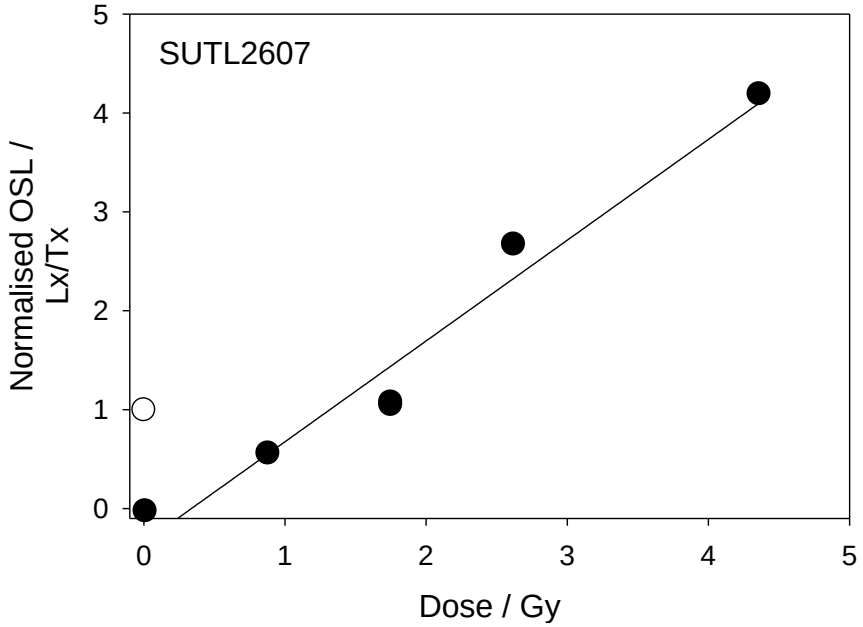

Fig C-10: Dose response for SUTL2607, 150-250 µm, 2.64-2.74 gcm^{-3} 40% HF-etched 'quartz' fraction;

Lx = 1, 2, 3 and 5 Gy; Tx = 2 Gy

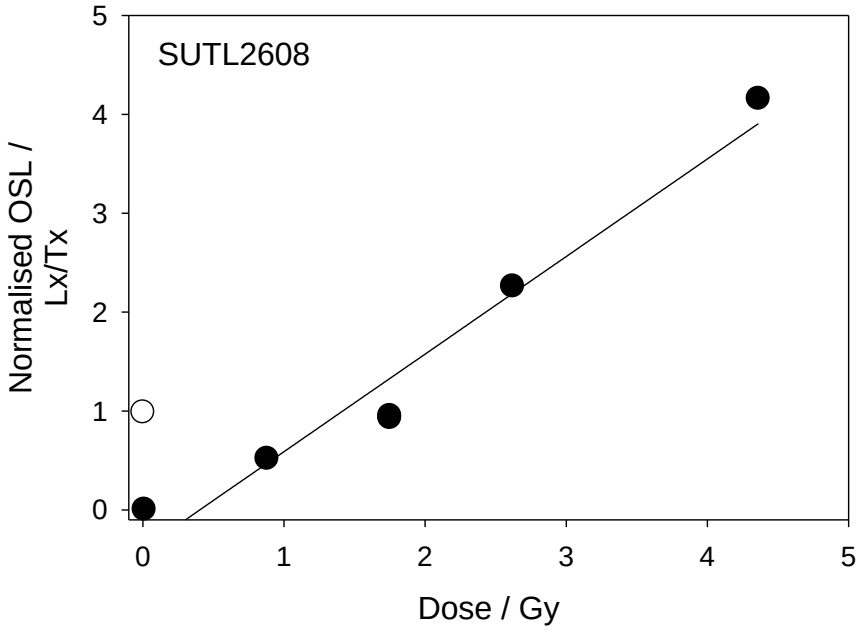

Fig C-11: Dose response for SUTL2608, 150-250 µm, 2.64-2.74 gcm^{-3} 40% HF-etched 'quartz' fraction;

Lx = 1, 2, 3 and 5 Gy; Tx = 2 Gy

Appendix D: Radial Plots

Fig D-1: Radial plot for SUTL2576

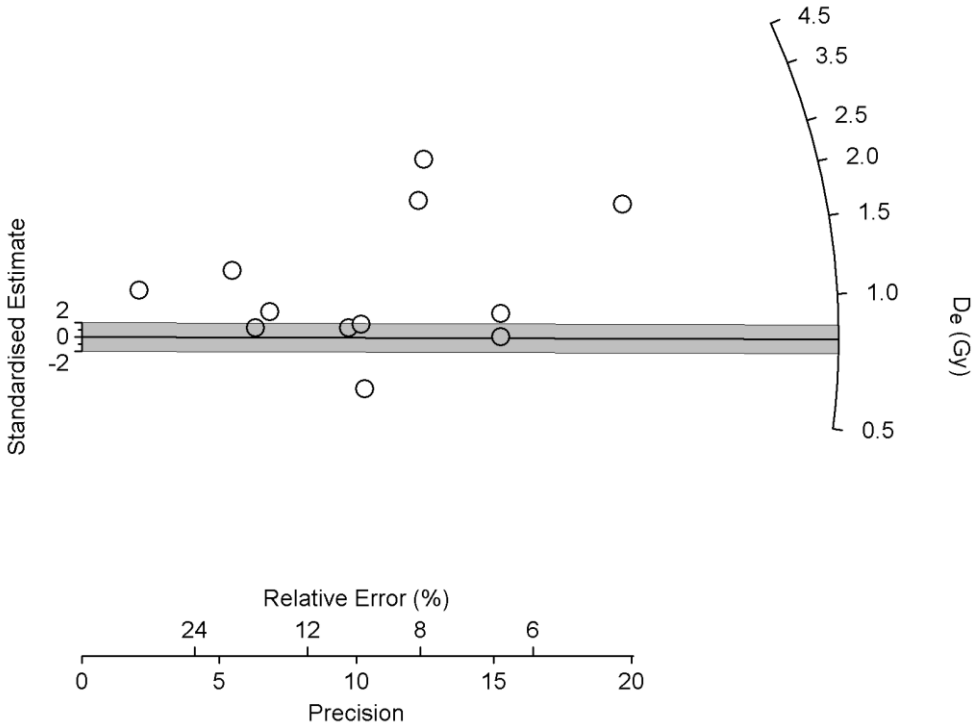

Fig D-2: Radial plot for SUTL2577

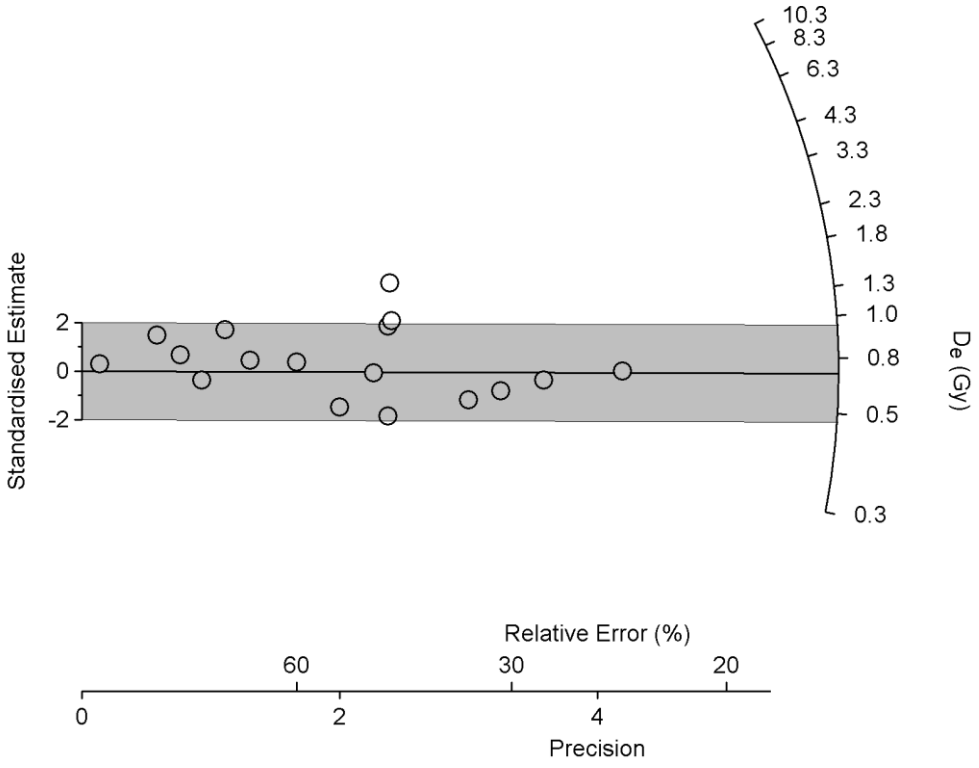

Fig D-3: Radial plot for SUTL2605

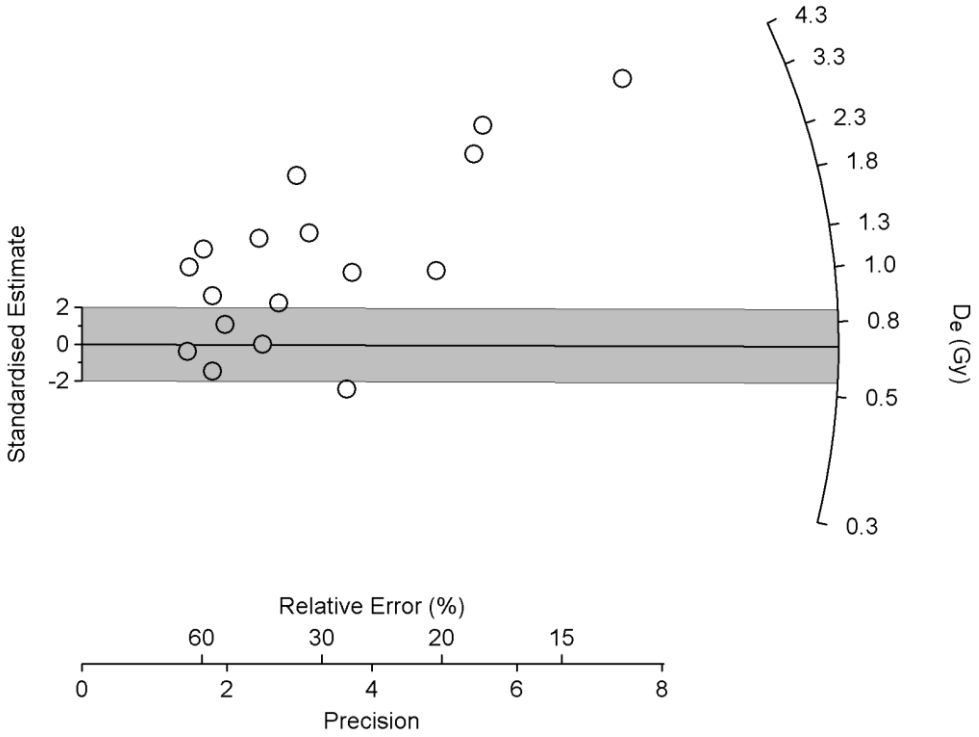

Fig D-4: Radial plot for SUTL2606

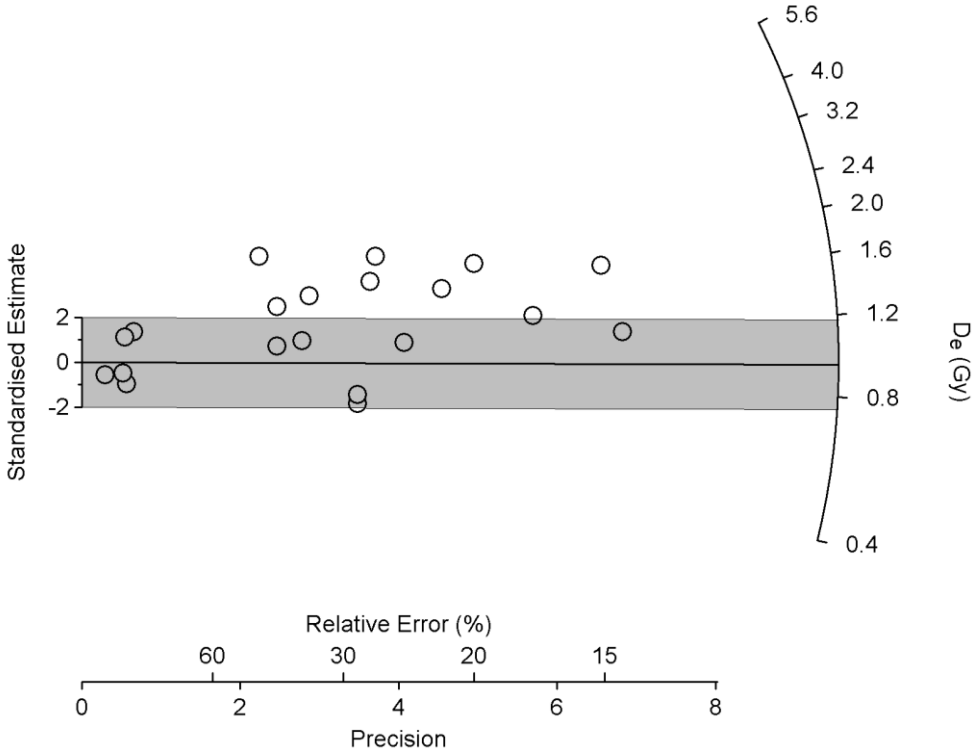

Fig D-5: Radial plot for SUTL2607

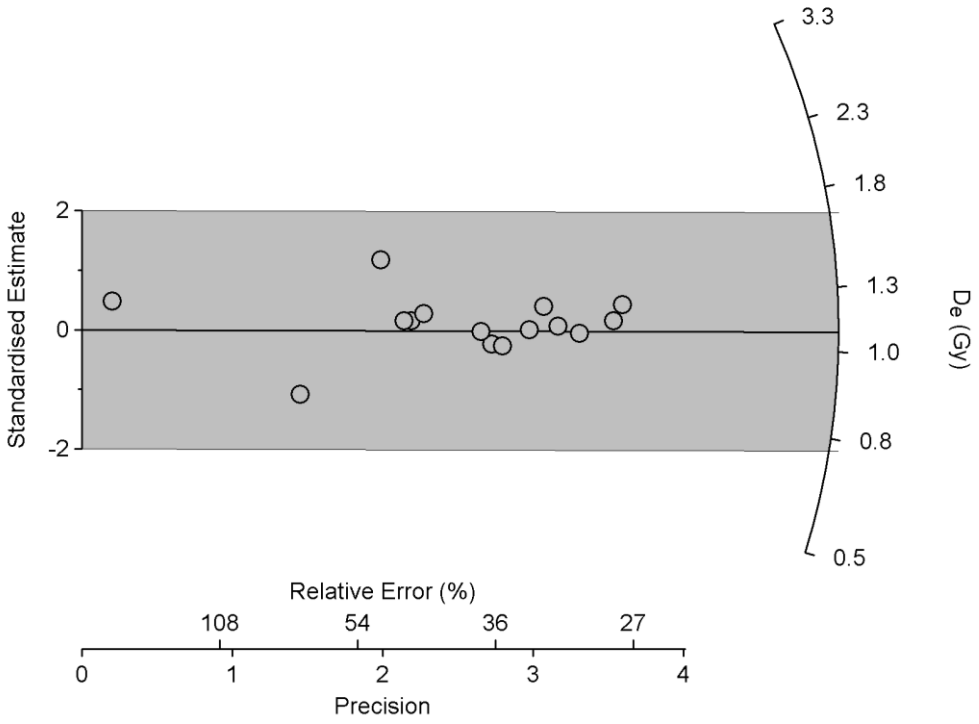

Fig D-6: Radial plot for SUTL2608

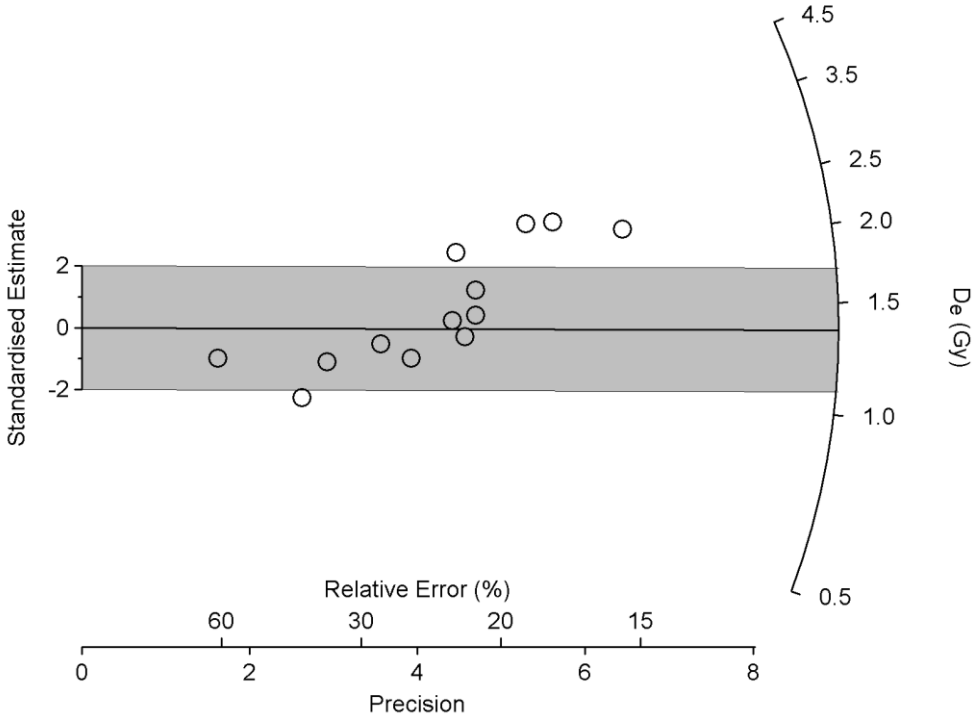

Appendix E: Dose rate determinations for SUTL2576 and 2577

SUTL no.	Depth / cm	Activity Concentration (Bq kg^{-1})[a]			Equivalent Concentration[b]		
		^{40}K	U	Th	K (%)	U (ppm)	Th (ppm)
2577C	-100	467 ± 16	27 ± 1	31 ± 1	1.51 ± 0.05	2.19 ± 0.11	7.55 ± 0.20
2577D	-105	521 ± 14	14 ± 1	29 ± 0	1.69 ± 0.05	1.13 ± 0.04	7.03 ± 0.12
2577E	-108	523 ± 16	21 ± 1	26 ± 1	1.69 ± 0.05	1.70 ± 0.09	6.38 ± 0.17
2577F	-116	550 ± 14	13 ± 0	25 ± 0	1.78 ± 0.05	1.07 ± 0.04	6.27 ± 0.10
2577G	-119	497 ± 12	15 ± 0	25 ± 0	1.61 ± 0.04	1.18 ± 0.03	6.22 ± 0.08
2577H	-125	550 ± 18	13 ± 1	28 ± 1	1.78 ± 0.06	1.08 ± 0.07	7.00 ± 0.19
2577I	-130	505 ± 13	33 ± 1	34 ± 0	1.63 ± 0.04	2.65 ± 0.09	8.42 ± 0.12
2577J	-139	522 ± 15	36 ± 2	39 ± 1	1.69 ± 0.05	2.95 ± 0.13	9.64 ± 0.22
2577K	-146	554 ± 16	30 ± 1	32 ± 1	1.79 ± 0.05	2.43 ± 0.12	7.97 ± 0.19
2576A	-155	489 ± 12	23 ± 1	27 ± 1	1.58 ± 0.04	1.84 ± 0.10	6.74 ± 0.21
2576B	-161	527 ± 19	24 ± 3	26 ± 2	1.70 ± 0.06	1.95 ± 0.22	6.52 ± 0.40
2576C	-164	592 ± 19	13 ± 2	20 ± 2	1.91 ± 0.06	1.07 ± 0.18	4.99 ± 0.42
2576D	-169	610 ± 16	13 ± 1	25 ± 1	1.97 ± 0.05	1.05 ± 0.10	6.16 ± 0.25
2576E	-176	482 ± 13	16 ± 1	20 ± 1	1.56 ± 0.04	1.27 ± 0.08	5.05 ± 0.20
2576F	-184	551 ± 12	14 ± 1	26 ± 1	1.78 ± 0.04	1.17 ± 0.07	6.35 ± 0.16
2576G	-192	542 ± 21	23 ± 3	30 ± 2	1.75 ± 0.07	1.83 ± 0.24	7.31 ± 0.48
2576H	-203	545 ± 21	12 ± 2	26 ± 2	1.76 ± 0.07	1.01 ± 0.20	6.44 ± 0.46

Table D-1:Activity and equivalent concentrations of K, U and Th determined by HRGS

[a]Shap granite reference, working values determined by David Sanderson in 1986, based on HRGS relative to CANMET and NBL standards.

[b]Activity and equivalent concentrations for U, Th and K determined by HRGS (Conversion factors based on NEA (2000) decay constants): 40K: 309.3 Bq kg^{-1} %K^{-1}, 238U: 12.35 Bq kg^{-1} ppmU^{-1}, 232Th: 4.057 Bq kg^{-1} ppm Th^{-1}

SUTL no.	Depth / cm	HRGS, dry (mGy a^{-1})[a]		
		Alpha	Beta	Gamma
2577C	-100	10.10 ± 0.31	1.77 ± 0.04	0.94 ± 0.02
2577D	-105	10.23 ± 0.68	1.89 ± 0.06	0.97 ± 0.04
2577E	-108	6.67 ± 0.58	1.89 ± 0.06	0.84 ± 0.03
2577F	-116	7.47 ± 0.34	1.97 ± 0.04	0.91 ± 0.02
2577G	-119	7.26 ± 0.26	1.62 ± 0.04	0.78 ± 0.02
2577H	-125	7.93 ± 0.23	1.83 ± 0.04	0.89 ± 0.01
2577I	-130	10.50 ± 0.76	1.93 ± 0.07	1.01 ± 0.04
2577J	-139	7.57 ± 0.65	1.80 ± 0.06	0.87 ± 0.02
2577K	-146	11.66 ± 0.33	1.79 ± 0.05	1.00 ± 0.02
2576A	-155	8.35 ± 0.14	1.77 ± 0.04	0.90 ± 0.01
2576B	-161	9.45 ± 0.27	1.84 ± 0.05	0.93 ± 0.02
2576C	-164	7.62 ± 0.13	1.81 ± 0.04	0.87 ± 0.01
2576D	-169	7.87 ± 0.10	1.68 ± 0.03	0.84 ± 0.01
2576E	-176	8.16 ± 0.23	1.83 ± 0.05	0.91 ± 0.02
2576F	-184	13.59 ± 0.26	1.98 ± 0.04	1.13 ± 0.02
2576G	-192	15.31 ± 0.41	2.11 ± 0.05	1.24 ± 0.02
2576H	-203	12.65 ± 0.35	2.07 ± 0.05	1.12 ± 0.02

Table D-2: Infinite matrix dose rates determined by HRGS and TSBC.

[a]based on dose rate conversion factors in Aikten (1983) and Sanderson (1987)

SUTL no.	depth / cm	distance from dating sample / r	weighting factor / $e^{-\mu r}$	gamma dose rate / mGy a^{-1}	gamma dose rate at sampling position/ mGy a^{-1}
2577A	-88	31	0.045	-	
2577B	-92	27	0.067	-	
2577C	-100	19	0.150	1.00 ± 0.02	
2577D	-105	14	0.247	0.90 ± 0.01	
2577E	-108	11	0.333	0.93 ± 0.02	
2577F	-116	3	0.741	0.87 ± 0.01	
2577G	**-119**	**0**	**1.000**	0.84 ± 0.01	**0.90 ± 0.01**
2577H	-125	6	0.549	0.91 ± 0.02	
2577I	-130	11	0.333	1.13 ± 0.02	
2577J	-139	20	0.135	1.24 ± 0.02	
2577K	-146	27	0.067	1.12 ± 0.02	
2576A	-155	29	0.055	0.94 ± 0.02	
2576B	-161	23	0.100	0.97 ± 0.04	
2576C	-164	20	0.135	0.84 ± 0.03	
2576D	-169	15	0.223	0.91 ± 0.02	
2576E	-176	8	0.449	0.78 ± 0.02	
2576F	**-184**	**0**	**1.000**	0.89 ± 0.01	**0.87 ± 0.01**
2576G	-192	8	0.449	1.01 ± 0.04	
2576H	-203	19	0.150	0.87 ± 0.02	
2576I	-224	40	0.018	-	

Table D-3: Scaling factors, weighted gamma dose rate estimates, and the calculated gamma dose rates received at each of the sampling positions (in bold)

SUTL No.	Water Content (%)			Effective Dose Rate (mGy a^{-1})		
	Fractional	Saturated	Assumed	Beta[a]	Gamma[b]	Total[c]
2576	4.5	19.2	12 ± 7	1.45 ± 0.11	0.90 ± 0.01	2.53 ± 0.11
2577	5.4	19.0	12 ± 7	1.33 ± 0.10	0.87 ± 0.01	2.39 ± 0.11

Table D-4: Water contents, and effective beta and gamma dose rates following water correction.

[a] Effective beta dose rate combining water content corrections with inverse grain size attenuation factors obtained by weighting the 200 μm attenuation factors of Mejdahl (1979) for K, U, and Th by the relative beta dose contributions for each source determined by Gamma Spectrometry.

[b] the sum of the gamma dose components obtained from stratigraphic layers in proximity to the dating sample, weighted relative to distance from the sample position

[c] Total dose rate from beta, gamma and cosmic components